



# Seasonal Changes in Dissolved Organic Matter Composition in a Patagonian Fjord Affected by Glacier Melt Inputs

Matthew G. Marshall<sup>1\*</sup>, Anne M. Kellerman<sup>2</sup>, Jemma L. Wadham<sup>1,3</sup>, Jon R. Hawkings<sup>2,4</sup>, Giovanni Daneri<sup>5</sup>, Rodrigo Torres<sup>5</sup>, Helena V. Pryer<sup>1</sup>, Alexander Beaton<sup>6</sup>, Hong Chin Ng<sup>7</sup>, Alejandra Urrea<sup>8</sup>, Laura F. Robinson<sup>7</sup> and Robert G. M. Spencer<sup>2</sup>

<sup>1</sup> Bristol Glaciology Centre, School of Geographical Sciences, University of Bristol, Bristol, United Kingdom, <sup>2</sup> Geochemistry Group, National High Magnetic Field Laboratory, Department of Earth, Ocean and Atmospheric Science, Florida State University, Tallahassee, FL, United States, <sup>3</sup> Centre for Arctic Gas Hydrate, Environment and Climate, Department of Geosciences, UiT The Arctic University of Norway, Tromsø, Norway, <sup>4</sup> German Research Centre for Geosciences GFZ, Potsdam, Germany, <sup>5</sup> Centro de Investigación en Ecosistemas de la Patagonia, Coyhaique, Chile, <sup>6</sup> Ocean Technology and Engineering Group, National Oceanography Centre, Southampton, United Kingdom, <sup>7</sup> School of Earth Sciences, University of Bristol, Bristol, United Kingdom, <sup>8</sup> Centro de Estudios Científicos, Valdivia, Chile

## OPEN ACCESS

### Edited by:

Angel Borja,  
Technological Center Expert in Marine  
and Food Innovation (AZTI), Spain

### Reviewed by:

Tzong-Yueh Chen,  
National Taiwan Ocean University,  
Taiwan

J. German Rodriguez,  
Technological Center Expert in Marine  
and Food Innovation (AZTI), Spain

### \*Correspondence:

Matthew G. Marshall  
mm5876@bristol.ac.uk

### Specialty section:

This article was submitted to  
Marine Ecosystem Ecology,  
a section of the journal  
Frontiers in Marine Science

**Received:** 30 September 2020

**Accepted:** 04 March 2021

**Published:** 09 April 2021

### Citation:

Marshall MG, Kellerman AM, Wadham JL, Hawkings JR, Daneri G, Torres R, Pryer HV, Beaton A, Ng HC, Urrea A, Robinson LF and Spencer RGM (2021) Seasonal Changes in Dissolved Organic Matter Composition in a Patagonian Fjord Affected by Glacier Melt Inputs. *Front. Mar. Sci.* 8:612386. doi: 10.3389/fmars.2021.612386

Biogeochemical processes in fjords are likely affected by changes in surrounding glacier cover but very little is known about how meltwater directly influences dissolved organic matter (DOM) in fjords. Moreover, the data available are restricted to a handful of northern hemisphere sites. Here we analyze seasonal and spatial variation in dissolved organic carbon (DOC) concentration and DOM composition (spectrofluorescence, ultrahigh resolution mass spectrometry) in Baker-Martinez Fjord, Chilean Patagonia (48°S), to infer the impacts of rapid regional deglaciation on fjord DOM. We show that surface layer DOC concentrations do not vary significantly between seasons, but DOM composition is sensitive to differences in riverine inputs. In summer, higher protein-like fluorescence reflects increased glacial meltwater inputs, whilst molecular level data show weaker influence from marine DOM due to more intense stratification. We postulate that the shifting seasonal balance of riverine and marine waters affects the supply of biolabile peptides and organic nitrogen cycling in the surface layer. Trends in DOM composition with increasing salinity are consistent with patterns in estuaries (i.e. preferential removal of aromatic compounds and increasing relative contribution of unsaturated and heteroatom-rich DOM from marine sources). Preliminary estimates also suggest that at least 10% of the annual organic carbon stock in this fjord is supplied by the four largest, glacially fed rivers and that these inputs are dominated by dissolved (84%) over particulate organic carbon. Riverine DOC may therefore be an important carbon subsidy to bacterial communities in the inner fjord. The overall findings highlight the biogeochemical sensitivity of a Patagonian fjord to changes in glacier melt input, which likely has relevance for other glaciated fjords in a warming climate.

**Keywords:** dissolved organic matter, Chilean Patagonia, FT-ICR MS, glacier melt, fjord biogeochemistry

## INTRODUCTION

Fjords are critical zones of fresh and marine water interaction (e.g., Bianchi et al., 2020), which support hotspots of ecological productivity (e.g., Iriarte et al., 2007) and important carbon sinks (e.g., Smith et al., 2015) in the mid- to high-latitudes. The biogeochemistry of fjords is thought sensitive to the effects of climate change, especially where the enhanced melting and long-term retreat of glaciers will lead to changes in the timing, magnitude and composition of freshwater inputs (Cuevas et al., 2019; Saldías et al., 2019). The impact of glacial meltwaters on fjord nutrient cycles has attracted much interest in recent years (Hawkings et al., 2014, 2016; Hopwood et al., 2020). However, we know very little about the direct influence of glaciers on dissolved organic matter (DOM) in fjords, especially beyond the effects on overall biolability and the fluorescent fraction (Paulsen et al., 2017, 2018). Focused analysis of the wider DOM pool via molecular methods, as offered by this study, can help to improve our understanding of how carbon cycling in fjords might be affected by accelerated glacier melting and eventual landscape deglaciation.

Dissolved organic matter is an important phase in the aquatic biogeochemical cycles of carbon and major nutrients (e.g., Burd et al., 2016) and its overall reactivity is strongly linked to its composition (Amon and Benner, 1994; Sun et al., 1997; Hopkinson et al., 1998; Mostovaya et al., 2017). In coastal waters, DOM comprises a complex mixture of material from marine and terrestrial sources, modified through biological and photochemical degradation (Hernes and Benner, 2003; Spencer et al., 2009; Ward et al., 2017) and physico-chemical removal mechanisms (Sholkovitz, 1976; Eisma, 1986; Keil et al., 1994; Aufdenkampe et al., 2001). Changes in the source and supply of DOM will have a profound effect on its composition, its role as an energy source to heterotrophic bacteria and its pathway through aquatic ecosystems (Pace et al., 2004; Welti et al., 2017). DOM cycling in fjords is therefore sensitive to major changes in the upstream landscape (Asmala et al., 2016; Ward et al., 2017), which is primarily driven by rapid rates of glacier retreat in large regions of the higher latitudes (Zemp et al., 2015).

Enhanced glacier melting will likely increase the supply of reactive DOM to fjords in the short term (Milner et al., 2017). This hypothesis rests upon evidence from bioincubation studies which show that DOM in glacial meltwaters is protein-rich, highly bioavailable and easily respired by downstream heterotrophs (Hood et al., 2009; Fellman et al., 2010; Singer et al., 2012; Lawson et al., 2014; Hemingway et al., 2019). Although few studies have directly assessed the impact in fjords, data from Young Sound, Greenland, suggest that glacial DOM may support offshore bacteria even when other sources of organic matter are more plentiful (Paulsen et al., 2017, 2018). Moreover, the incorporation of glacial organic carbon into the biomass of higher organisms in land-based systems highlights a potential to support complex food webs in fjords (Hågvar and Ohlson, 2013; Fellman et al., 2015). The supply of biolabile DOM in meltwaters will decline as glaciers recede in the long term and more stable terrestrial organic matter is mobilized from expanding proglacial zones

(Milner et al., 2017; Paulsen et al., 2017; Hemingway et al., 2019). However, more detailed analysis of DOM composition in glacially influenced fjords is needed to better understand its sensitivity to predicted changes in meltwater supply and the overall impact on fjord biogeochemistry.

The formation of DOM by primary production in fjords is also sensitive to changing glacier influences. For example, marine-terminating glaciers can sustain highly productive ecosystems via hydrodynamic controls on nutrient supply (Meire et al., 2017). Upwellings of deeper nutrient-rich waters, which stimulate primary productivity at the surface, might shut down when submarine meltwater discharge ceases as glaciers retreat onto land (Hopwood et al., 2018). Primary productivity is limited further by reduced light transmission through the water column as turbid meltwaters get redirected to the fjord surface (Aracena et al., 2011). Under such conditions, DOM derived from glacial and terrestrial sources may play a greater role in carbon cycling by microbial food webs at the heads of the fjords (González et al., 2013).

Chilean Patagonia contains an extensive network of fjords that are fed by rivers draining near-pristine catchments with variable glacier cover (Pantoja et al., 2011). The region contains the largest volume of land ice in the southern hemisphere outside Antarctica (Millan et al., 2019), concentrated in two major icefields which are melting rapidly (Glasser et al., 2011; Foresta et al., 2018). Accelerated melting is increasing freshwater flux to the coast in this region (Dussailant et al., 2019), with implications for fjord hydrodynamics and the supply of organic matter (Iriarte et al., 2014). Freshwater flux is driven primarily by summertime melting but, in contrast to fjords in polar regions, heavy precipitation sustains year-round freshwater inputs and above-freezing sea level temperatures support a more limited amount of glacial melting in winter (Rebolledo et al., 2019). Understanding how fjord DOM composition responds to seasonal changes in freshwater source (intense glacial melting in summer and heavier precipitation in winter) is relevant for glacially influenced fjords in other wet, maritime locations, such as New Zealand and the Gulf of Alaska, contrasting with polar fjords where freshwater inputs are driven almost exclusively by melt cycles.

Here we present DOC concentration and detailed DOM composition data (determined via fluorescence analysis and ultrahigh resolution mass spectrometry) from the heavily glaciated Baker-Martinez Fjord (BMF) in Chilean Patagonia. We compare summer and winter DOM composition in the surface layer to subsurface conditions across seasons within a single year to infer changes in DOM source and in-fjord processing within the context of changing glacier melt inputs. We apply molecular level techniques that have advanced understanding of DOM in temperate estuarine settings (Osterholz et al., 2016; Seidel et al., 2017) to enhance the interpretation of fjord DOM beyond the relatively small fluorescent fraction, which has been the focus of the few studies in glaciated fjords so far (Paulsen et al., 2018). We aim to: (i) assess the impact of glacier melt inputs on fjord DOM composition by comparing summer (high melt) and winter (low melt) conditions; (ii) examine variations in DOM molecular composition along the salinity gradient to elucidate

environmental controls and infer biogeochemical processes; and (iii) conduct a preliminary assessment of the relative importance of riverine inputs to the organic matter pool in the BMF.

## MATERIALS AND METHODS

### Study Region

The BMF is situated between the Northern and Southern Patagonian Icefields (NPI, SPI) at  $\sim 48^\circ\text{S}$  (Figure 1) and consists of two largely disconnected sub-basins: the northerly Martinez Channel (typically  $< 500$  m deep) and the deeper (up to  $\sim 1075$  m) Baker Channel to the south (Piret et al., 2019). Strong freshwater inputs from several glacier-fed rivers and high annual rainfall maintain a stratified water column typical of fjords, with a freshwater lens sitting above higher salinity waters (Rebolledo et al., 2019). Vertical exchange between the two layers is largely controlled by semidiurnal tides (Ross et al., 2014), whilst the prevailing westerly winds drive the general circulation patterns in the fjord (Aiken, 2012), such as subsurface warm water intrusions from Baker Channel into Jorge Montt Fjord (Moffat, 2014). Freshwater inputs peak with river discharge in the austral summer (December–March) due to seasonal glacier melting rather than with maximum rainfall in the austral winter (May–August) (Rebolledo et al., 2019). The regimes of the largest rivers, the Baker and Pascua, are dominated by melting of the NPI and SPI, respectively (Dirección General de Aguas, 2019). Discharge from the Huemules River, driven primarily by melting of Steffen Glacier, NPI, and direct meltwater inputs from Jorge Montt Glacier, SPI, are not well quantified at present. The Bravo River, at the head of Mitchell Fjord, is less influenced by meltwaters from smaller mountain glaciers. Strong turbid meltwater inputs lead to light limitation and relatively low levels of primary productivity in BMF ( $49\text{--}840$  mg C  $\text{m}^{-2}$   $\text{d}^{-1}$ ), when compared to Chilean fjords between  $44$  and  $47^\circ\text{S}$  ( $1667\text{--}2616$  mg C  $\text{m}^{-2}$   $\text{d}^{-1}$ ), where glacial cover and meltwater inputs are much lower (Aracena et al., 2011; González et al., 2011; Jacob et al., 2014).

### Sampling

Fjord water samples were collected during research cruises in the austral summer (16–23 February) and winter (4–9 July) of 2017. A RBRmaestro or RBRconcerto CTD was deployed from the *RV Sur Austral* to obtain water column profiles of temperature, salinity, turbidity and chlorophyll fluorescence at each station (Figure 1). Water was sampled from selected depths (approximately 1, 5, 50, 150, and 250 m as water depth and conditions allowed) using a standard 10 L Niskin bottle or a 10 L Go-Flo bottle (General Oceanics). Where logistically possible, the same stations were revisited in winter to capture seasonal differences. Exceptions include the summer stations in Jorge Montt Fjord (S12 and S13) where floating ice mélangé restricted access in winter to one alternative site (S20), and an additional winter station near the mouth of the Baker Channel (S21) which could not be accessed in summer due to rough conditions. An underway sampling system, comprising a Teflon diaphragm pump and custom-made epoxy coated “torpedo” (towfish) that extended 2 m from the side of the ship was deployed during

passage between stations to capture variations in the surface layer ( $\sim 1.5$  m depth) at higher spatial resolution.

River samples were collected from the Baker River (in summer; Figure 1 site D) and rivers in the Huemules valley (both seasons; Figure 1 sites A–C) during complementary land-based sampling campaigns. Samples were collected from the mouth of the Baker in winter (Figure 1, site D) and the Bravo (Figure 1, site E) and Pascua (Figure 1, site F) rivers in both seasons during the fjord surveys. Although the Baker, Bravo and Pascua rivers were sampled only once per season, collectively these samples establish a baseline of DOM composition from the major rivers emptying into the BMF.

### Analytical Methods

#### Dissolved Organic Carbon (DOC) and Nutrient Concentrations

Samples for DOC measurement were filtered to  $0.45$   $\mu\text{m}$  using either Whatman® Polycap GW PES filter capsules (fjord surface samples), Geotech Versapor filter capsules (fjord subsurface samples) or Whatman® Puradisc AQUA syringe filters (river samples) and stored frozen in acid-clean HDPE bottles (Nalgene®). DOC concentrations were determined for all fresh and marine water samples on a Shimadzu TOC-L<sub>CHN</sub> analyzer equipped with the saline sample kit (e.g., Kellerman et al., 2020). The limits of detection ( $\text{LoD} = \text{LoB} + [1.645 \times \text{SD of low concentration sample}]$ ; where  $\text{LoB} = \text{limit of blank}$ ) and quantification ( $\text{LoQ} = \text{LoB} + [5 \times \text{SD of low concentration sample}]$ ) were calculated as  $2.7$   $\mu\text{M}$  and  $3.7$   $\mu\text{M}$ , respectively (Armbruster and Pry, 2008). Repeat measurement of a  $40$   $\mu\text{M}$  standard varied by  $< \pm 5\%$ .

Samples for dissolved nutrient analysis were filtered to  $0.45$   $\mu\text{m}$  using either Whatman® Polycap GW PES filter capsules (fjord surface sample) or Whatman® GD/XP dpPP syringe filters (river samples/fjord samples at depth) and stored frozen in acid-clean HDPE bottles (Nalgene®). Concentrations of ammonium ( $\text{NH}_4^+$ ), nitrate ( $\text{NO}_3^-$ ), nitrite ( $\text{NO}_2^-$ ), total dissolved nitrogen (TDN), dissolved organic nitrogen (DON), and soluble reactive phosphorus (SRP;  $\text{PO}_4^{3-}$ ) were measured on a LaChat QuikChem® 8500 series 2 flow injection analyzer using established colorimetric methods, with matrix matched standards (e.g., Hawkings et al., 2015). DON concentrations were taken as the difference between TDN, measured following an alkaline persulfate/UV digestion at  $120^\circ\text{C}$  to convert all DON to  $\text{NO}_3^-$  (Hosomi and Sudo, 1986) with alterations for saline samples, and the sum of inorganic nitrogen forms ( $\text{NH}_4^+ + \text{NO}_3^- + \text{NO}_2^-$ ) measured prior to digestion. Digest efficiency was checked with organic N spiked samples and standards. LoDs were  $0.10$   $\mu\text{M}$ ,  $0.07$   $\mu\text{M}$ , and  $0.03$   $\mu\text{M}$  for DON,  $\text{NO}_3^-$  and SRP, respectively, with a precision  $< \pm 5\%$  for  $\text{NO}_3^-$  and SRP and  $< \pm 15\%$  for DON.

#### DOM Fluorescence Analysis

Dissolved organic matter samples for fluorescence analysis were collected in the same way as for DOC concentration. Excitation-emission matrices (EEMs) were collected on an Agilent Cary Eclipse Fluorescence Spectrophotometer with xenon flash bulb. Scans were conducted in  $10$  mm quartz cuvettes over excitation wavelengths  $240\text{--}450$  nm at  $5$  nm intervals and emission

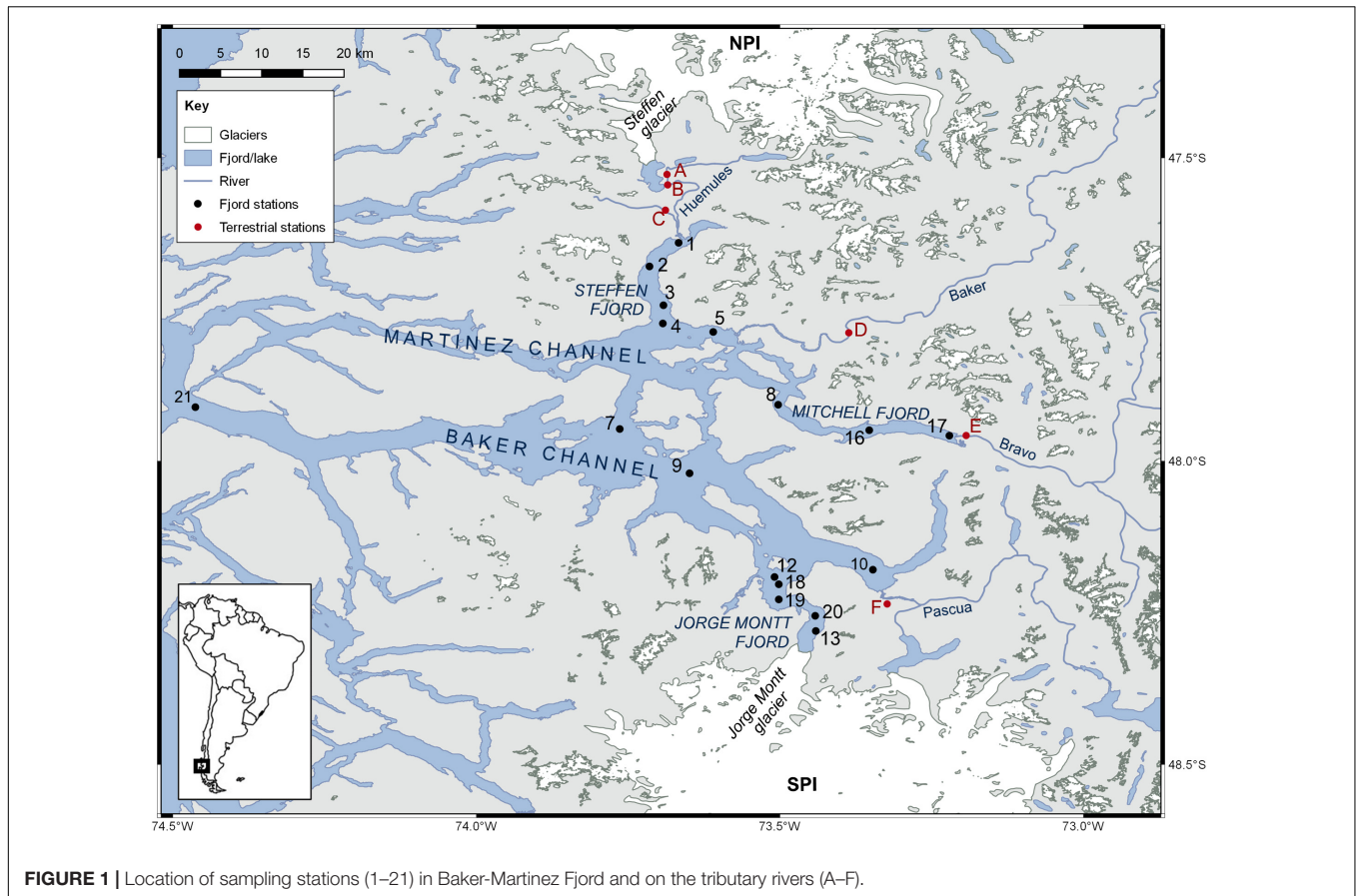


**FIGURE 1** | Location of sampling stations (1–21) in Baker-Martinez Fjord and on the tributary rivers (A–F).

wavelengths 300–600 nm at 2 nm intervals, using 5 nm monochromator slit widths and 0.1 s integrations. All EEMs were corrected for instrumental biases and Raman/Rayleigh scatter prior to subsequent analysis (Murphy et al., 2013).

### Ultrahigh Resolution Mass Spectrometry

Large volume (1 L) samples were filtered through either PES capsule filters (0.45  $\mu\text{m}$ ; as above for fjord surface samples) or pre-combusted (450°C, 5 h) GF/Fs (nominally 0.7  $\mu\text{m}$ ; all Steffen valley, summer Baker River and fjord water column samples) into pre-cleaned polycarbonate bottles (10% HCl for 24 h followed by copious rinsing with 18.2  $\text{M}\Omega\text{ cm}^{-1}$  ultra-pure water) and acidified to pH  $\sim$ 2 with analytical grade HCl. Filtered samples were solid phase extracted (SPE) onto 200 mg Varian Bond Elut PPL cartridges following established protocols (Dittmar et al., 2008). Based on DOC measurements for each sample, the SPE-DOM was eluted with methanol to obtain a target concentration of  $\sim$ 60  $\mu\text{g C ml}^{-1}$ .

Analyses were conducted on a custom built 21 tesla Fourier transform ion cyclotron resonance mass spectrometer (FT-ICR MS) at the National High Magnetic Field Laboratory (NHMFL) (Smith et al., 2018). Samples were introduced via electrospray ionization (2.6–3.2 kV) at a rate of 600  $\text{nl min}^{-1}$  and analyzed in negative ion mode. Mass spectra for each sample were derived from 100 coadded scans and calibrated against known  $m/z$  values using Predator software (NHMFL).

Formulae were assigned to all peaks with mass calibration errors  $<$  500 ppb and intensities 6 times greater than the RMS signal to noise ratio plus baseline (PetroOrg software, Florida State University) using stoichiometric combinations within the range of  $\text{C}_{1-45}\text{H}_{1-92}\text{N}_{0-4}\text{O}_{1-25}\text{S}_{0-2}$ . All assigned formulae were categorized into compound groups based on elemental ratios and values of the modified aromaticity index ( $\text{AI}_{\text{mod}}$ ; Koch and Dittmar, 2006) using the following classification scheme: condensed aromatics (CA;  $\text{AI}_{\text{mod}} > 0.66$ ); polyphenolics (PP;  $0.66 \geq \text{AI}_{\text{mod}} > 0.5$ ); highly unsaturated and phenolic (HUP;  $\text{AI}_{\text{mod}} \leq 0.5$ ;  $\text{H/C} < 1.5$ ); aliphatic ( $2 \geq \text{H/C} \geq 1.5$ ;  $\text{N} = 0$ ); peptide-like ( $2 \geq \text{H/C} \geq 1.5$ ;  $\text{N} > 0$ ) and sugar-like ( $\text{H/C} > 1.5$ ;  $\text{O/C} > 0.9$ ) (Kellerman et al., 2018). Further subdivisions include low and high O/C ratios ( $<$ 0.5 or  $>$ 0.5) for HUPs and aliphatics.

### Particulate Organic Carbon Concentrations

Particulate organic carbon (POC) concentrations were measured from large volume (1–3 L) grab samples collected from each of the four largest tributary rivers entering the BMF. POC samples were not collected at fjord stations. Particles were retained on pre-combusted (450°C, 5 h) GF/F filters (Whatman®), which were then dried and analyzed directly through high temperature (1000°C) catalytic combustion on a Thermo Electron Flash Elemental Analyzer 1110. Organic carbon (OC) content was determined following removal of inorganic carbon by acidification (Hedges and Stern, 1984). All samples

were corrected for the filter blank, assessed as  $0.03 \pm 0.01\%$  for total carbon (TC) and  $0.02 \pm 0.01\%$  for OC ( $n = 10$ ). The % OC content was converted to POC concentration using the suspended sediment concentration (SSC), which was determined as the mass of dry sediment retained on pre-weighed membrane filters from a known volume of water ( $\sim 300$  ml).

## Flux Calculations

We estimate the magnitudes of DOC and POC fluxes from the four principal rivers as cumulative annual discharge multiplied by mean DOC or POC concentrations. Annual discharge for the Baker and Pascua rivers is well constrained by long-term records from the Chilean Water Authority (Dirección General de Aguas, 2019). We also make use of the first discharge data for the Huemules River, derived from a stage-discharge rating curve ( $r^2 = 0.97$ ; RMSE  $< \pm 9\%$ ) based on pressure sensor readings from a stable bedrock position within the river and 14 Rhodamine wt dye injection traces over the austral summer and winter in 2017 (Bartholomew et al., 2011). Only an estimate of the average annual discharge of the Bravo River was available (Aracena et al., 2011).

## Statistical Methods

Multi-way DOM fluorescence data was decomposed into separate components using parallel factor (PARAFAC) analysis with the drEEM Toolbox for MATLAB (Murphy et al., 2013). The dataset contained 407 EEMs, including samples from the BMF ( $n = 129$ ), its tributary rivers ( $n = 102$ ) and additional freshwater and marine bodies ( $n = 176$ ) from the broader study region ( $42\text{--}48^\circ\text{S}$ ). A seven-component PARAFAC model, which explained  $> 98.6\%$  of variance across all samples, was found to fit the data best following inspection of residuals and use of split-half validation. All model components matched components in the OpenFluor database (Murphy et al., 2014).

All other statistical tests were performed in R (R Core Team, 2015). Non-parametric Mann Whitney tests (for unpaired, non-normally distributed data) were used to assess the significance of seasonal differences in water column structure, bulk geochemistry and FT-ICR MS data at the compound category level. Mann Whitney tests were also used to test differences between the fjord surface and subsurface layers. Molecular level relationships with water column properties and season were tested using Spearman rank correlations between the relative intensities of individual formulae present in all fjord samples and CTD data; correlations with season were tested by means of a dummy variable (i.e., summer = 0; winter = 1). Raw  $p$ -values  $< 0.028$  for these correlations were deemed significant at the 95% confidence interval following a false discovery rate correction (Benjamini and Hochberg, 1995), which minimizes the number of false positive (Type I) errors arising from the large number of tests for  $\sim 18,000$  formulae. The relationships between salinity variations and FT-ICR MS relative intensities for major compound categories were also assessed using Spearman rank correlation tests.

Principal Components Analysis (PCA) was applied to a dataset comprising normalized FT-ICR MS compound category relative intensities (%) and PARAFAC fluorescence loadings (%)

for each fjord sample, to assess variation in DOM composition across the fjord samples. All variables were first standardized between 0 and 1 using the *decostand* function in the R vegan package (Oksanen et al., 2016). Multivariate correlations between the ordination (PCA) results and water column properties were assessed by permutation ( $n = 999$ ) using the *envfit* function (Oksanen et al., 2016).

## RESULTS

### Seasonality in Fjord Water Column Properties and Chemical Composition

The physical properties of the BMF water column display marked seasonality, with significantly lower salinities (Mann Whitney;  $p < 0.001$ ) and higher turbidity ( $p < 0.05$ ) linked to a thicker ( $p < 0.01$ ) freshwater layer in summer. Surface temperatures are higher in summer ( $p < 0.01$ ) despite strong meltwater input, except near the head of Steffen Fjord (S1 and S2) where winter warming coincides with the largest increase in surface salinity across the study area (Table 1).

The chemical composition of the surface layer also varies seasonally. Dissolved nutrients ( $\text{NO}_3$ , SRP) mostly fall below the analytical LoD in summer but reach detectable concentrations in winter (Table 1). This coincides with increased surface chlorophyll concentrations in winter ( $p < 0.01$ ). Nutrient concentrations show limited variability in the surface layer but increase exponentially with salinity, reaching maximum subsurface concentrations of  $\sim 25 \mu\text{M}$  and  $\sim 2 \mu\text{M}$  for  $\text{NO}_3$  and SRP, respectively. However, nutrient concentrations are highly variable at salinities  $> 25$  (Supplementary Figure 1).

Surface DOC concentrations are highly variable across the BMF ( $\sim 20\text{--}200 \mu\text{M}$ ) and seasonal differences (summer =  $85.7 \pm 41.1 \mu\text{M}$ ; winter =  $72.1 \pm 33.1 \mu\text{M}$ ; mean  $\pm$  SD) are not statistically significant (Figure 2A). Subsurface DOC is generally less variable (summer =  $56.5 \pm 8.5 \mu\text{M}$ ; winter =  $41.7 \pm 4.3 \mu\text{M}$ ) but the seasonal difference is significant ( $p < 0.001$ ). Spatial variations in surface DOC are largely controlled by differences in river inputs (Supplementary Figures 2a,b), with the highest concentrations in Mitchell Fjord linked to outflow from the organic-rich Bravo River. The lowest surface DOC concentrations are in Steffen Fjord near the mouth of the Huemules River (Figure 1 and Table 1), which is dominated by glacial meltwater inputs.

Surface DON concentrations are generally low in summer and increase in winter (Figure 2B). The difference is only statistically significant ( $p < 0.05$ ) when the Baker and Pascua River plumes (S5 and S10, respectively), which show little seasonal change (Table 1), are excluded from the analysis. This suggests that the wintertime increase in fjord surface DON concentrations is not linked to changes in the major rivers. Patterns in Jorge Montt Fjord deviate from the general trend, as surface DON concentrations are higher in summer ( $3.6 \mu\text{M}$  at S13, vs.  $2.4 \mu\text{M}$  at S20 in winter; Table 1). DON concentrations are highly variable but, in general, are lower at lower salinity (Figure 2B). Variation in DON largely controls the N/C molar ratio, which generally increases with salinity, with two high

**TABLE 1** | Physical and chemical properties of surface layer and selected subsurface depths at survey stations in Baker-Martinez Fjord in austral summer (February) and austral winter (July) 2017.

Station	Sample depth (m)	Freshwater depth (m)		Salinity		Temperature (°C)		Turbidity (NTU)		Chlorophyll (µg/L)		DOC (µM)		DON (µM)		N/C (molar ratio)		NO <sub>3</sub> (µM)		SRP (µM)		
		Feb	Jul	Feb	Jul	Feb	Jul	Feb	Jul	Feb	Jul	Feb	Jul	Feb	Jul	Feb	Jul	Feb	Jul	Feb	Jul	
<b>Surface Lens</b>																						
<b>Martinez Channel &amp; Inlets</b>																						
Steffen Fjord	S1	1	4.2	0.7	1.6	16.4	4.9	6.8	60.0	9.7	0.192	0.975	36.6	21.2	1.1	3.4	0.030	0.161	0.34	3.04	< 0.03	0.39
	S2	1	6.5	4.7	1.3	13.1	4.7	6.2	63.7	11.2	0.235	0.683	49.0	64.8	1.1	5.1	0.023	0.079	0.33	0.57	< 0.03	0.37
	S3	1	7.7	–	1.2	–	7.4	–	59.5	–	0.215	–	–	–	–	–	–	–	–	–	–	–
	S4	1	7.6	3.4	1.2	5.6	10.4	5.8	29.1	15.6	0.312	1.066	39.3	64.8	2.4	3.5	0.061	0.054	0.08	1.18	< 0.03	0.12
Baker plume	S5	1	5.0	3.0	0.5	0.7	11.6	5.9	93.5	32.9	0.226	0.484	44.1	61.9	1.9	1.7	0.043	0.028	< 0.07	0.50	< 0.03	0.27
Mitchell Fjord	S17	1	6.0	5.3	0.4	1.9	9.3	3.7	32.0	9.9	0.500	1.005	199.7	188.3	2.9	3.7	0.014	0.020	0.21	0.89	< 0.03	0.03
	S16	1	8.6	5.7	0.6	3.3	12.4	4.0	15.7	12.9	0.567	1.144	130.8	110.1	2.0	3.2	0.015	0.029	< 0.07	1.18	< 0.03	0.26
	S8	1	7.7	4.4	0.9	4.7	13.0	4.4	20.1	10.3	0.394	1.032	128.3	166.8	3.6	5.1	0.028	0.030	< 0.07	0.84	< 0.03	0.10
<b>Baker Channel &amp; Inlets</b>																						
Jorge Montt Fjord	S13	1	8.2	–	2.1	–	4.9	–	3.0	–	0.966	–	60.0	–	3.6	–	0.063	–	< 0.07	–	<0.03	–
	S20	1	–	8.6	–	6.7	–	2.1	–	4.2	–	1.140	–	52.7	–	2.4	–	0.046	–	1.18	–	0.10
	S12	1	8.2	–	2.0	–	7.1	–	4.4	–	0.963	–	60.6	–	3.8	–	0.060	–	< 0.07	–	<0.03	–
Pascua plume	S10	1	5.0	5.5	1.1	5.9	8.8	4.9	30.4	7.4	0.296	0.892	46.0	58.0	2.3	2.2	0.049	0.038	0.53	1.30	0.04	0.20
Central fjord	S7	1	6.8	3.8	0.8	7.2	11.6	5.8	51.2	12.1	0.385	0.795	60.9	95.6	1.9	3.2	0.031	0.033	0.07	1.96	< 0.03	0.30
	S9	1	7.8	6.2	2.5	13.2	11.0	6.3	8.8	2.3	0.652	0.897	77.3	65.3	2.0	2.7	0.026	0.041	< 0.07	2.91	< 0.03	0.28
Outer fjord	S21	1	–	3.1	–	16.0	–	6.4	–	1.1	–	0.972	–	67.2	–	6.9	–	0.103	–	0.83	–	0.44
<b>Subsurface</b>																						
Steffen Fjord	S1	40	–	–	–	31.9	–	11.4	–	0.4	–	0.053	–	41.9	–	7.6	–	0.182	–	8.78	–	1.06
	S4	270	–	–	–	33.9	–	8.2	–	0.5	–	0.035	–	36.7	–	7.5	–	0.204	–	19.06	–	1.92
Baker plume	S5	140	–	–	–	33.7	–	8.9	–	0.7	–	0.044	–	45.9	–	1.6	–	0.036	–	21.13	–	1.72
Mitchell Fjord	S17	130	–	–	–	33.7	–	8.8	–	0.4	–	0.087	–	74.9	–	7.4	–	0.098	–	17.78	–	1.35
Jorge Montt Fjord	S20	30	–	–	–	30.7	–	8.9	–	49.9	–	0.073	–	43.1	–	5.3	–	0.123	–	8.28	–	0.90
	S20	180	–	–	–	31.5	–	10.8	–	0.9	–	0.048	–	47.5	–	7.0	–	0.147	–	5.35	–	0.96
Baker Channel	S9	180	–	–	–	33.8	–	8.4	–	0.2	–	0.021	–	38.8	–	9.0	–	0.233	–	20.56	–	1.76

Subsurface data presented only for depths from which samples were collected for FT-ICR MS analysis in winter.

anomalies at intermediate salinities ( $\sim 16$ ) in winter samples from near the mouth of the Baker Channel (S21) (**Figure 2C** and **Supplementary Figure 2f**).

## Trends in DOM Composition

### DOM Fluorescence

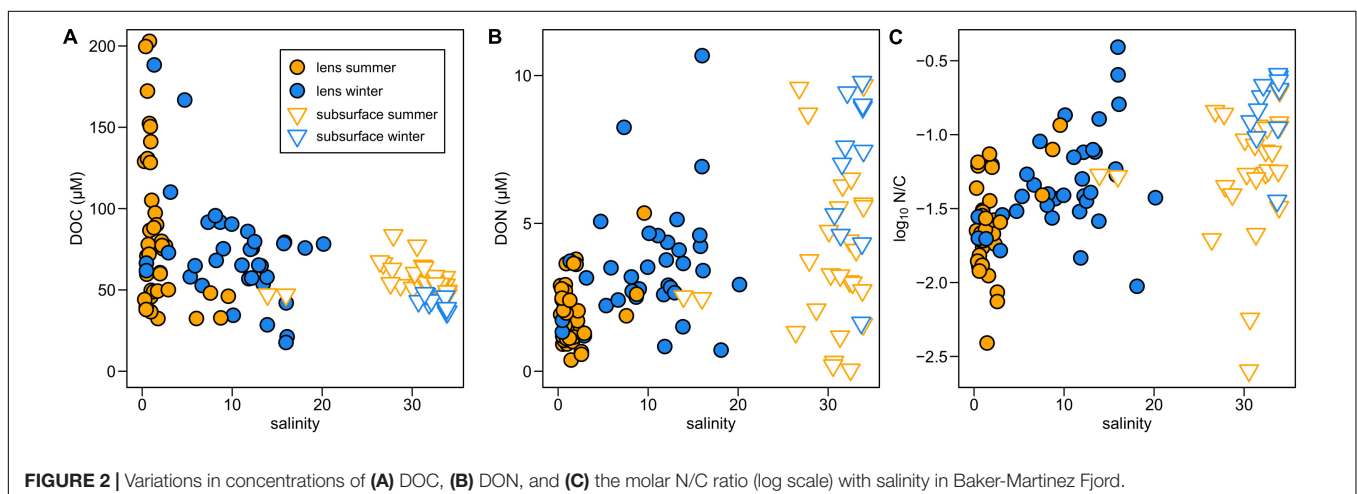
The PARAFAC model identified three terrestrial humic-like ( $C_{498}$ ,  $C_{452}$ ,  $C_{446}$ ), one marine humic-like ( $C_{390}$ ) and three protein-like fluorophores ( $C_{304}$ ,  $C_{328}$ ,  $C_{354}$  – the latter being tryptophan-like) (**Supplementary Table 1**). Humic-like fluorescence intensity is directly correlated with DOC concentrations but inversely correlated with salinity and N/C ratios (**Figure 3**). The same relationships exist for two protein-like fluorophores ( $C_{328}$ ,  $C_{354}$ ) but with weaker correlations (**Figure 3**). The other protein-like component ( $C_{304}$ ) does not vary systematically with any of these variables (**Figure 3**).

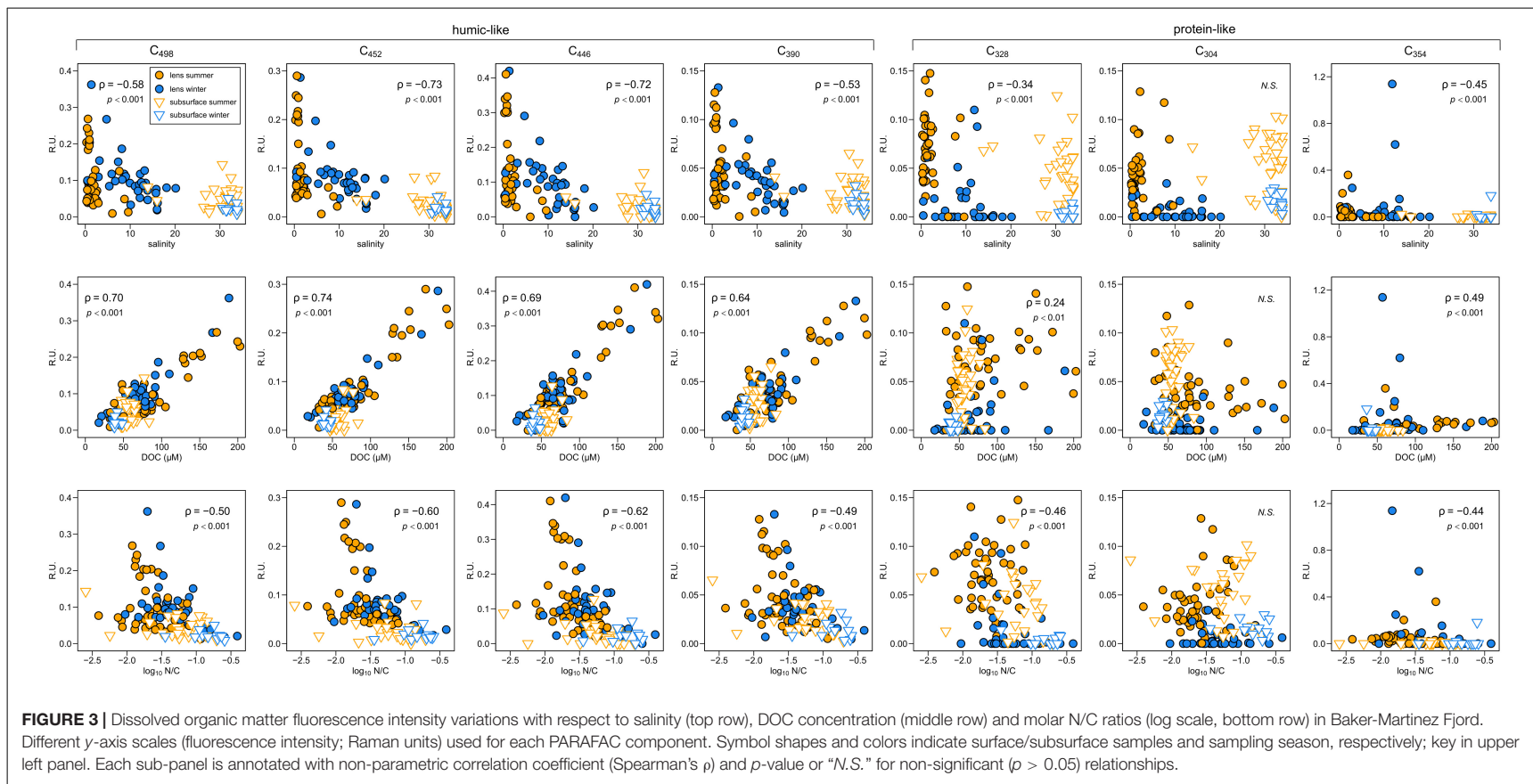
Surface layer fluorescence intensities are similar in both seasons for most PARAFAC components, except for protein-like  $C_{328}$  and  $C_{304}$ , which are found at significantly lower intensities in winter (Mann Whitney,  $p < 0.001$ ). Generally, fluorescence intensities in the fjord surface layer are similar to the rivers for all components, except  $C_{304}$  which has significantly lower intensity in the fjord in winter ( $p < 0.05$ ). Spatial variations in surface layer humic-like fluorescence correspond to DOC concentration patterns and largely reflect compositional variability of riverine inputs (**Supplementary Figures 2a,b, 3a,b**). Protein-like fluorescence intensity is generally lower but local spikes, which are mostly driven by increases in  $C_{354}$  (up to 1.2 R.U.), occur at intermediate salinities ( $\sim 13$ ) near the mouth of Jorge Montt Fjord, in the upper Martinez Channel and (where data are available in winter only) the mid-Baker Channel (**Supplementary Figures 3c–f**). This suggests potential sources of  $C_{354}$  in the fjord. However, summertime intensities of  $C_{354}$  are 0.03–0.09 R.U. in the rivers (mean  $\pm$  SD =  $0.05 \pm 0.03$  R.U.,  $n = 6$ ) but this drops to zero in the surface layer of Steffen Fjord (S1, S2, and S4), near the head of Martinez Channel (S5), and in Baker Channel (S7, S9, and S10), suggesting possible consumption of this component.

### Molecular Composition

A total of 18,383 unique formulae in the mass range of 175–1000 Da were identified in 26 fjord and 8 river samples of SPE-DOM. Of these, 5,321 (28.9%) were common to all fjord samples and 2,870 (15.6%) were exclusive to the fjord. Only 976 formulae (5.3%) were found exclusively in river samples and these were mostly aliphatic or HUPs. HUPs comprise the bulk of all formulae ( $72.1 \pm 3.1\%$ ) and sample intensities ( $83.7 \pm 5.5\%$ ), including in the N-containing fraction ( $78.9 \pm 4.5\%$  of formulae and  $84.5 \pm 6.4\%$  of intensity). The mean relative intensities of other major compound groups listed in descending order were PP ( $9.6 \pm 4.4\%$ ), aliphatic ( $3.6 \pm 0.8\%$ ), CA ( $2.5 \pm 1.2\%$ ), sugar-like ( $0.3 \pm 0.2\%$ ), and peptide-like ( $0.3 \pm 0.2\%$ ). There were no significant differences between the rivers and the fjord surface layer when comparing formulae counts or relative intensities for each compound category. However, the subsurface waters had higher relative intensities of HUP ( $p = 0.001$ ) and peptide-like ( $p < 0.05$ ) formulae, but lower relative intensities of PP ( $p = 0.001$ ), CA ( $p < 0.01$ ), and sugar-like ( $p < 0.01$ ) formulae than surface waters. The fjord surface layer exhibited an increase in HUP ( $p < 0.05$ ) and decrease in PP ( $p < 0.05$ ) relative intensities from summer to winter.

The molecular composition of fjord DOM displays a marked transition with salinity, reflecting differences in compound group relative intensities between seasons in the surface layer and the subsurface (**Figure 4**). The general relationship shows a decline in more aromatic compounds (PP, CA) and an increase in HUPs with increasing salinity. Aliphatics show no discernible trend with salinity, whereas peptide-like compounds increase with salinity. Correlations between individual formulae and environmental variables confirm that PP and CA compounds are associated with less saline and more turbid conditions — characteristic of the surface layer, where they are relatively more enriched in summer (**Table 2**). The HUP and aliphatic fractions in the surface layer display a shift from more O-rich formulae in summer to more O-poor formulae in winter, with the O-poor formulae more strongly associated with more saline, higher chlorophyll, and less turbid conditions (**Table 2**).





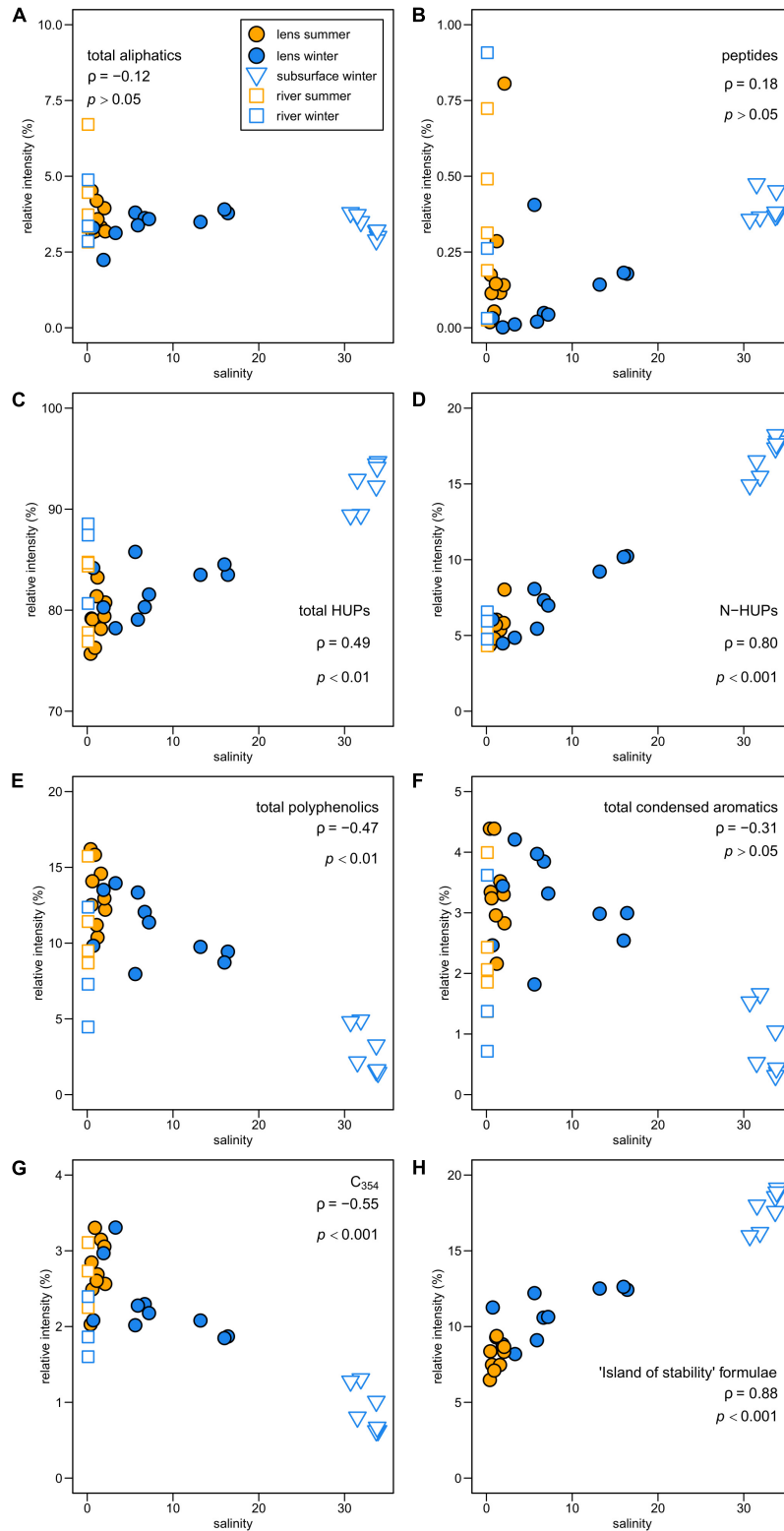
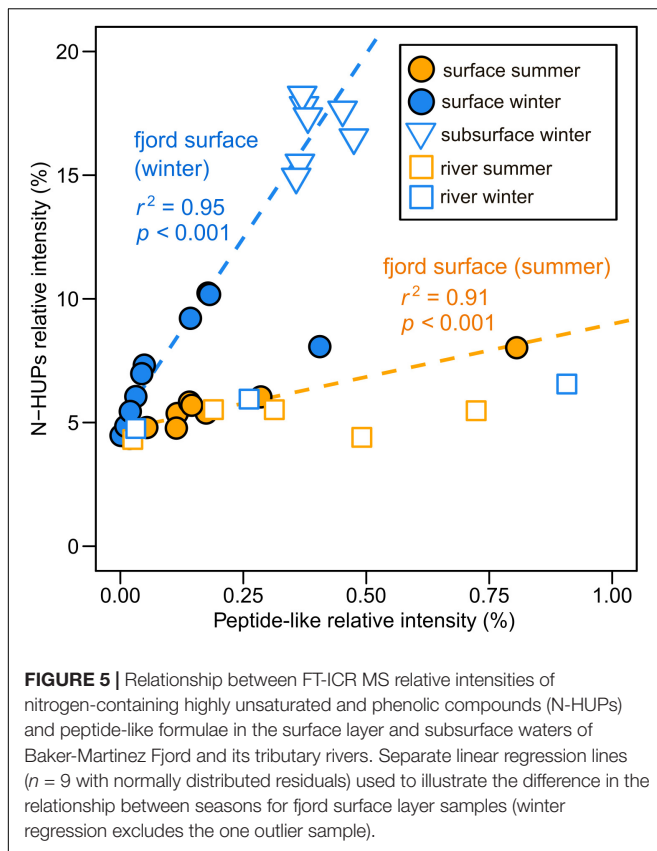


**FIGURE 4** | Relationship between FT-ICR MS compound category relative intensities and salinity in Baker-Martinez Fjord for **(A)** aliphatic, **(B)** peptide-like, **(C)** all HUPs, **(D)** N-HUPs, **(E)** polyphenolic and **(F)** condensed aromatic formulae. Sub-panel **(G)** shows variations in formulae correlated with tryptophan-like ( $C_{354}$ ) fluorescence in river samples across the broader region; and **(H)** shows variations in formulae from a stable pool of marine DOM, termed the “island of stability” (Lechtenfeld et al., 2014). Sub-panels annotated with non-parametric correlation coefficient (Spearman’s  $\rho$ ) and  $p$ -value where  $p > 0.05$  is not deemed significant. River samples excluded from correlations but shown for reference.

**TABLE 2** | Characteristics of FT-ICR MS-derived formulae that are significantly correlated (Spearman rank,  $p$ -value < 0.028) with season and water column properties in Baker-Martinez Fjord.

		Season		Salinity		Chlorophyll		Turbidity	
		Summer	Winter	Higher salinity	Lower salinity	Higher chlorophyll	Lower chlorophyll	Higher turbidity	Lower turbidity
<b>Number of correlated formulae</b>		1770 ± 27	2075 ± 45	2942 ± 196	4334 ± 118	4075 ± 105	2453 ± 185	3624 ± 89	2445 ± 169
<b>Intensity-weighted molecular properties of correlated formulae</b>	mass	476.6 ± 2.3	464.4 ± 1.0	451.0 ± 0.6	498.9 ± 2.7	521.1 ± 2.1	446.6 ± 0.7	492.4 ± 3.0	448.4 ± 0.6
	C	20.8 ± 0.1	22.8 ± 0.1	20.9 ± 0.0	22.4 ± 0.1	24.9 ± 0.1	19.9 ± 0.0	22.0 ± 0.1	20.7 ± 0.0
	H	20.1 ± 0.1	28.3 ± 0.1	26.0 ± 0.0	20.3 ± 0.1	25.1 ± 0.3	24.9 ± 0.0	19.8 ± 0.1	25.8 ± 0.0
	O	13.0 ± 0.1	10.0 ± 0.0	10.6 ± 0.0	13.1 ± 0.1	12.3 ± 0.1	11.1 ± 0.0	13.0 ± 0.1	10.6 ± 0.0
	N	0.03 ± 0.00	0.12 ± 0.01	0.21 ± 0.01	0.05 ± 0.00	0.05 ± 0.00	0.25 ± 0.02	0.05 ± 0.00	0.23 ± 0.02
	S	0.01 ± 0.00	0.06 ± 0.00	0.08 ± 0.00	0.01 ± 0.00	0.02 ± 0.00	0.08 ± 0.00	0.02 ± 0.00	0.08 ± 0.00
	H/C	0.97 ± 0.01	1.24 ± 0.00	1.25 ± 0.00	0.91 ± 0.01	0.99 ± 0.01	1.25 ± 0.00	0.91 ± 0.01	1.25 ± 0.00
	O/C	0.63 ± 0.00	0.44 ± 0.00	0.51 ± 0.00	0.59 ± 0.00	0.50 ± 0.01	0.56 ± 0.00	0.60 ± 0.00	0.51 ± 0.00
	N/C	0.00 ± 0.00	0.01 ± 0.00	0.01 ± 0.00	0.00 ± 0.00	0.00 ± 0.00	0.01 ± 0.00	0.00 ± 0.00	0.01 ± 0.00
	Almod	0.36 ± 0.00	0.26 ± 0.00	0.22 ± 0.00	0.42 ± 0.00	0.40 ± 0.01	0.20 ± 0.00	0.42 ± 0.00	0.22 ± 0.00
<b>Relative intensities of correlated formulae by compound category (%)</b>	Aliph. O-rich	0.22 ± 0.02	0.00 ± 0.00	0.65 ± 0.04	0.13 ± 0.01	0.00 ± 0.00	0.83 ± 0.04	0.15 ± 0.01	0.39 ± 0.03
	Aliph. O-poor	0.16 ± 0.02	0.19 ± 0.01	0.30 ± 0.01	0.80 ± 0.05	1.17 ± 0.06	0.23 ± 0.01	0.65 ± 0.05	0.19 ± 0.01
	Peptide	0.06 ± 0.01	0.01 ± 0.00	0.10 ± 0.02	0.00 ± 0.00	0.00 ± 0.00	0.15 ± 0.02	0.00 ± 0.00	0.09 ± 0.02
	HUP O-rich	20.33 ± 1.14	10.53 ± 0.72	24.43 ± 1.66	22.43 ± 1.47	8.40 ± 0.68	23.86 ± 1.59	21.39 ± 1.44	21.96 ± 1.59
	HUP O-poor	0.53 ± 0.03	22.95 ± 0.85	16.21 ± 0.94	3.92 ± 0.19	12.34 ± 0.57	4.90 ± 0.47	2.96 ± 0.14	13.58 ± 0.88
	HUP with N	0.02 ± 0.00	1.20 ± 0.17	2.44 ± 0.38	0.14 ± 0.01	0.12 ± 0.00	2.16 ± 0.36	0.11 ± 0.01	2.37 ± 0.37
	PP O-rich	3.20 ± 0.26	0.00 ± 0.00	0.00 ± 0.00	7.28 ± 0.61	5.07 ± 0.45	0.00 ± 0.00	7.02 ± 0.59	0.00 ± 0.00
	PP O-poor	0.76 ± 0.05	0.02 ± 0.00	0.04 ± 0.01	2.16 ± 0.15	1.73 ± 0.12	0.02 ± 0.00	2.07 ± 0.14	0.03 ± 0.00
	PP with N	0.01 ± 0.00	0.01 ± 0.00	0.02 ± 0.00	0.07 ± 0.00	0.06 ± 0.00	0.01 ± 0.00	0.07 ± 0.00	0.01 ± 0.00
	CA O-rich	0.27 ± 0.03	0.01 ± 0.00	0.00 ± 0.00	2.27 ± 0.19	2.18 ± 0.19	0.00 ± 0.00	1.62 ± 0.13	0.00 ± 0.00
	CA O-poor	0.01 ± 0.00	0.00 ± 0.00	0.00 ± 0.00	0.11 ± 0.01	0.10 ± 0.01	0.00 ± 0.00	0.07 ± 0.00	0.00 ± 0.00
	CA with N	0.00 ± 0.00	0.00 ± 0.00	0.00 ± 0.00	0.00 ± 0.00	0.00 ± 0.00	0.00 ± 0.00	0.00 ± 0.00	0.00 ± 0.00
	Sugars	0.02 ± 0.00	0.00 ± 0.00	0.04 ± 0.01	0.17 ± 0.02	0.14 ± 0.02	0.04 ± 0.01	0.16 ± 0.02	0.01 ± 0.00

The characteristics of directly and inversely correlated formulae are split across the two columns per variable (corresponding to summer/winter for season, or higher/lower values for other variables). Results are reported as the mean ± 1 SE across all samples ( $n = 26$ , except for "season" correlations where only surface layer samples were included and  $n = 19$ ) for the number of correlated formulae, their (intensity-weighted) molecular properties and percentage relative intensities of specific compound categories (Aliph., aliphatics; HUP, highly unsaturated and phenolic; PP, polyphenolic; CA, condensed aromatics). Very small standard errors are reported as zero when mean values are also close to zero.



N-containing formulae in fjord DOM comprise a greater share of surface layer sample intensity in winter and are correlated directly with salinity but inversely with chlorophyll and turbidity (Table 2). This pattern is driven primarily by changes in N-HUPs. The relative intensities of all N-containing formulae, and N-HUPs exclusively, are directly correlated with DON concentrations (both give Pearson's  $r = 0.89$ ;  $p < 0.001$ ) when excluding one outlier sample (S5, depth 140 m, winter) from the analysis. Peptide-like formulae are a comparatively minor constituent of DON and display a weaker correlation with DON concentrations ( $r = 0.55$ ;  $p < 0.01$ ). Overall, surface layer peptide-like formulae intensities increase in summer, whereas N-HUPs intensities decrease (Table 2).

The relationship between peptide-like and N-HUP relative intensities differs between the seasons, with surface layer conditions more closely resembling the rivers in summer and the fjord subsurface in winter (Figure 5). The molecular properties of peptide-like formulae also differ significantly between rivers and the fjord surface layer over the seasons with respect to the fjord subsurface, as shown by a one-way multivariate analysis of variance (MANOVA; Pillai's trace = 0.19;  $F$ -test = 60.2; and  $p < 0.001$ ) of the molecular properties (continuous dependent variables) across sample types (independent factor variable) in Table 3. Higher relative intensities of peptide-like formulae in the fjord surface layer in summer (Figure 5) and overall association of peptide-like formulae with more saline/less turbid conditions (Table 2) that characterize winter, suggest multiple controls over peptide-like material in the fjord.

## Multivariate Relationships

Multivariate (PCA) analysis reveals relative variations in fjord DOM composition that are linked to the season and water depth (Figure 6). The first three PCA components explain 72.7% of the variance in the dataset. PC1 distinguishes surface layer DOM (richer in CAs and PPs and correlated with higher DOC concentrations) from subsurface DOM (characterized by higher relative intensities of O-rich HUPs and correlated with higher salinities, DON and nutrient concentrations). Subsurface samples (positive PC1 scores) are also associated with higher  $C_{304}$  (protein-like) and  $C_{390}$  (marine humic-like) fluorescence loadings.

PC2 reflects seasonal differences in surface layer DOM. Positive PC2 scores are associated with summer samples, characterized by higher protein-like fluorescence loadings, higher relative intensities of O-rich aliphatics and peptide-like compounds and directly correlated with turbidity and water temperature. Negative PC2 scores associated with winter samples reflect higher humic-like fluorescence loadings, higher relative intensities of O-poor HUPs and O-poor aliphatics and strong direct correlation with chlorophyll.

The relationship between PC2 and PC3 suggests a convergence in DOM composition across much of the fjord surface in winter, characterized by higher  $C_{390}$  fluorescence and O-poor HUPs/aliphatics (Figure 6B). In contrast, surface samples span greater compositional space in summer, with samples from Jorge Montt Fjord, and the Baker and Pascua plumes relatively enriched in protein-like fluorescence, O-rich aliphatics and peptides, whereas Steffen and Mitchell Fjords are enriched in O-rich HUPs (Figure 6B).

## Estimating River Fluxes

We estimate that the four principal rivers draining into BMF supply  $> 42$  Gg of organic carbon each year, with  $> 84\%$  as DOC and  $< 16\%$  as POC (Table 4). Despite turbid inputs, the low organic content ( $< 0.4\%$ ) of suspended sediments means that POC comprises a smaller share (2–32%) of total OC export than DOC (68–98%) in all rivers. The Baker River is the biggest single input of freshwater and OC, accounting for approximately half of the total annual flux. The next largest input from the Pascua River provides 38% of the freshwater and 26% of the OC from rivers each year. The Bravo River's OC flux is disproportionately high for its size due to high DOC concentrations; its annual DOC flux is similar to the Pascua River, which has an annual discharge at least six times larger. The dilute and predominantly NPI-fed Huemules River provides modest shares of the total freshwater (6%) and OC (2%) fluxes.

## DISCUSSION

### Seasonality in DOM Composition in Fjord Surface Layer

Seasonal changes in the fjord surface layer reflect a shifting balance between marine and freshwater influences that are linked to variations in river discharge and glacier melt cycles. The overall freshening, higher turbidity and low nutrient content in summer (Table 1) is consistent with strong meltwater input

**TABLE 3** | Comparison of properties of peptide-like formulae detected in FT-ICR MS spectra from river, fjord surface and fjord subsurface water samples in Baker-Martinez Fjord.

Properties of peptide-like formulae	Rivers		Fjord surface layer		Fjord subsurface
	Summer ( <i>n</i> = 5)	Winter ( <i>n</i> = 3)	Summer ( <i>n</i> = 9)	Winter ( <i>n</i> = 10)	Winter ( <i>n</i> = 7)
No. of formulae	157 ± 38	180 ± 96	118 ± 27	76 ± 25	314 ± 20
Rel. intensity (%)	0.34 ± 0.12	0.40 ± 0.26	0.21 ± 0.08	0.11 ± 0.04	0.40 ± 0.02
Mass (Da)	499.4 ± 4.8	500.2 ± 4.6	493.8 ± 4.5	468.2 ± 4.5	464.1 ± 3.7
H/C	1.60 ± 0.01	1.61 ± 0.00	1.60 ± 0.00	1.57 ± 0.00	1.58 ± 0.00
O/C	0.61 ± 0.01	0.61 ± 0.01	0.59 ± 0.01	0.55 ± 0.01	0.57 ± 0.01
N	1.64 ± 0.05	1.56 ± 0.04	1.24 ± 0.03	1.20 ± 0.03	1.37 ± 0.03
S	0.06 ± 0.01	0.00 ± 0.00	0.06 ± 0.01	0.24 ± 0.02	0.31 ± 0.02

Values are means ± 1 SE for samples of the same type, showing the number of peptide-like formulae, their share of sample relative intensity (%), formula mass (Da), H/C, O/C, and numbers of N and S atoms in each peptide-like formula.

from glaciers (Marin et al., 2013; Aracena et al., 2015; Hawkings et al., 2015). Weaker glacial melting in winter leads to increased surface salinities and nutrient concentrations (Table 1) as marine influences strengthen in the upper fjord layers, potentially enhanced by greater mixing with subsurface waters during winter storms (Montero et al., 2017). Seasonal cycles in freshwater input also control changes in the composition of surface layer DOM, with implications for its overall reactivity and biogeochemical fate. We discuss, in turn, three mechanisms relating to changes in freshwater input that affect DOM composition in BMF.

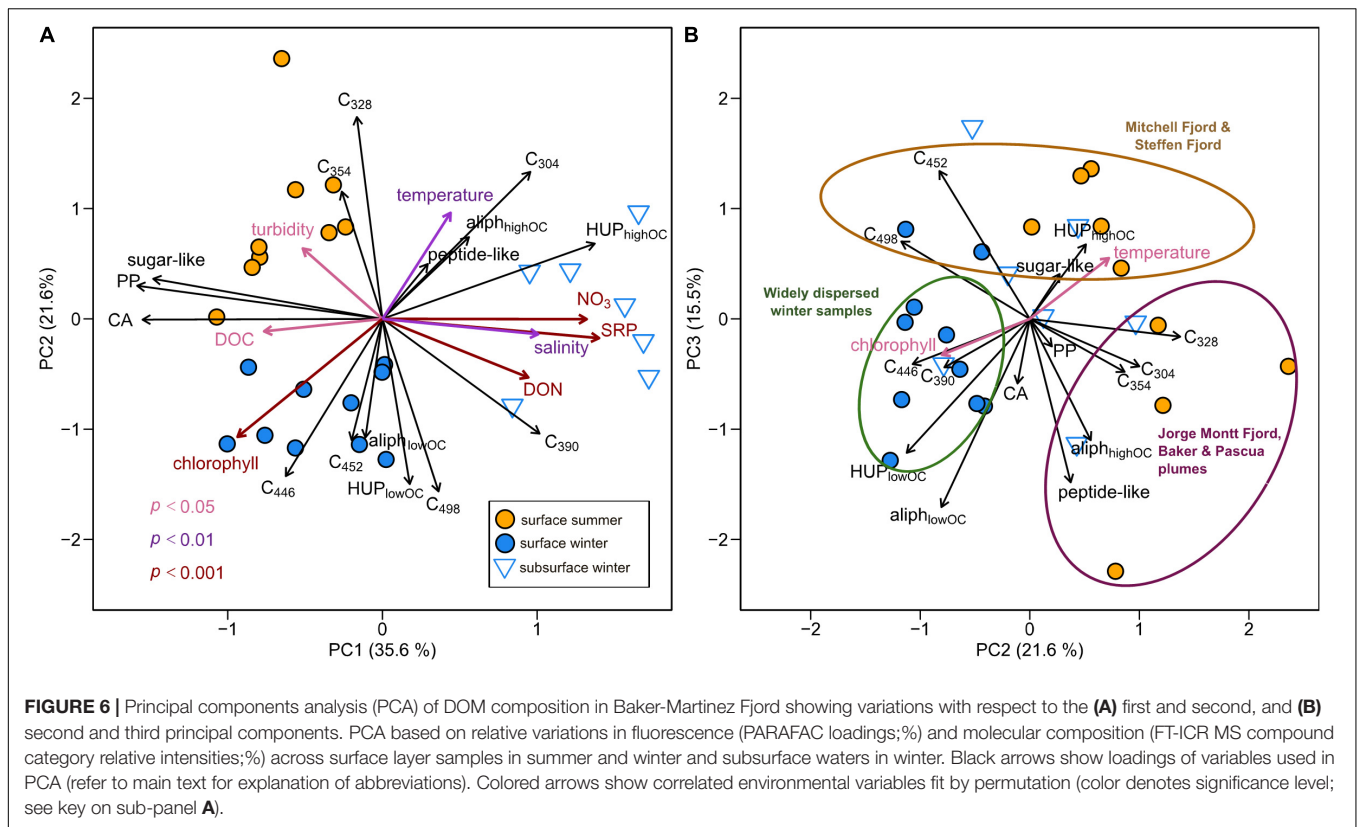
First, seasonal changes in freshwater DOM composition are transferred directly into the fjord surface layer. For example, higher protein-like fluorescence in summer (Figure 3) is consistent with strong meltwater inputs supplying DOM from glacial sources (Barker et al., 2006; Dubnick et al., 2010; Fellman et al., 2010; Kellerman et al., 2020). This is particularly evident downstream of Jorge Montt Glacier and near the mouths of the Baker and Pascua Rivers (Figure 6B), where summer discharge is driven by melting of the NPI and SPI, respectively (Dussaillant et al., 2012; Rebolledo et al., 2019). Protein-like fluorescence intensity decreases as meltwater inputs decline in winter (Figure 3). Higher surface layer humic-like fluorescence loadings in winter (Figure 6A) are consistent with more dominant non-glacial inputs, likely driven by heavier rainfall and increased flushing of vegetated terrain, soils and wetlands (Koch et al., 2005; Fellman et al., 2008, 2014; Ohno et al., 2010). Such DOM sources may dominate the River Bravo year round, as it is a less glacially influenced catchment. The year-round presence of humic-like fluorescence, PPs and CAs and their associations with higher DOC concentrations (Figures 3, 6A), suggest continuous inputs of terrestrial DOM via rivers and runoff from the highly vegetated banks of BMF.

Second, river discharge magnitude regulates the degree of mixing between fresh and marine waters in the surface layer. High discharge in summer accounts for higher protein-like fluorescence (Figure 3) from glacial meltwaters and increased relative intensities of PPs, which are derived from vascular plants and indicative of stronger terrestrial inputs (Riedel et al., 2016). Reduced glacial melting, weaker river discharge and greater turbulence in the fjord results in a thinner freshwater lens in winter, leading to higher surface salinities (Table 1) and increased

relative intensities of HUPs (Figure 4). In particular, greater N-HUP relative intensities in winter are consistent with the higher heteroatom (i.e., N) content of marine DOM (Sleighter and Hatcher, 2008; Osterholz et al., 2016). Moreover, the coincident increases in surface nutrient concentrations (Table 1) and inverse correlation between N-HUPs and chlorophyll (Table 2) indicate that these N-HUPs are likely sourced from subsurface waters rather than recently produced DOM near the surface, which is consistent with reduced stratification of the water column in winter.

Third, changes in the turbidity of freshwater inputs regulate primary production and the formation of autochthonous DOM in the fjord surface layer. Higher turbidity levels and greater stratification associated with strong glacial melt inputs suppress summertime primary production in BMF (Aracena et al., 2011). As meltwater inputs decline and turbidity levels fall in winter (Table 1), light is less limiting to the fjord ecosystem and primary production becomes a more important source of DOM. This accounts for the stronger association of O-poor aliphatics and HUPs with the winter surface layer (Figure 6A and Table 2) and, combined with the direct correlation of these compounds with chlorophyll (Table 2), is consistent with DOM derived from recent production by phytoplankton (Sleighter and Hatcher, 2008; Kujawinski et al., 2009; Landa et al., 2014). This molecular pool contrasts with the O-rich aliphatics and HUPs that are more strongly associated with the summer surface layer (Figure 6A and Table 2), and suggestive of stronger terrestrial influences when primary production is suppressed.

These seasonal shifts in surface layer DOM composition could affect how organic matter is processed by bacterial communities in BMF throughout the year. In summer, meltwater inputs likely support the bacterial cycling of bioavailable, protein-rich DOM from glacial sources (Hood et al., 2009; Fellman et al., 2014). This may be the dominant pathway for bacterial carbon cycling, especially where autochthonous DOM production is limited by high turbidity at the fjord heads (González et al., 2013) and where cold, low salinity conditions offer a competitive advantage to bacteria that are better adapted to glacial DOM (Gutiérrez et al., 2015; Paulsen et al., 2018). In contrast, bacterial activity may become increasingly coupled to autochthonous DOM sources as light becomes less limiting with decreased



discharge (Montero et al., 2011). However, the increased supply of relatively unreactive HUPs from subsurface waters may constrain the overall reactivity of surface layer DOM in winter (Mostovaya et al., 2017).

### Seasonality in N-Containing DOM

Dissolved organic matter biolability in the fjord may be most sensitive to changes in the N-containing fraction (i.e., DON). The strong correlation between DON concentrations and N-HUPs, which comprise the majority of all N-containing formulae and have higher intensities in the winter surface layer (Figure 4 and Table 1), suggests that the DON pool is dominated by refractory compounds from subsurface waters. The availability of peptide material, a small but biolabile fraction of DON (Aluwihare et al., 2005; Mulholland and Lee, 2009), may therefore exert a critical control over the reactivity of N-containing DOM in the fjord surface layer. The reduced number and lower N-content of peptide-like formulae in the fjord surface layer with respect to both riverine and subsurface sources (Table 3), suggest possible consumption of the most N-rich peptides. This effect is stronger in winter when there may be greater uptake by phytoplankton as increased light availability stimulates productivity (Mulholland and Lee, 2009).

Significant differences in peptide-like formulae across water sources (MANOVA,  $p < 0.001$ ; Table 3) suggest that biolabile nitrogen sources in the fjord surface layer could be sensitive to changes in the balance of marine and freshwater influences. Similarities between peptide-like formulae in the

surface layer in summer support a dominance of freshwater-derived peptide material (Table 3), with glaciers and proglacial lakes likely to be major sources (Spencer et al., 2014). Seasonal shifts in the composition of surface layer peptide-like formulae and their relationship with N-HUPs intensity (Figure 5 and Table 3) suggest an increased supply of peptide material from subsurface waters in winter, although rivers may continue to be an important local control in the near-shore zone (e.g., Supplementary Figure 5). The impacts of these changes in the supply of peptide material should, however, be viewed within the context of overall ecosystem productivity. When productivity is low in summer, organic N consumption might be limited to the bacterial uptake of biolabile, freshwater peptide material (González et al., 2013). Higher productivity in winter could lead to a greater total uptake by phytoplankton and bacteria, potentially supporting the co-metabolism of more stable subsurface peptide material alongside recent material from *in situ* production (Aluwihare et al., 2005; Aluwihare and Meador, 2008).

Our data contrast with previous studies of estuarine and marine DOM that identify proteins as a key component of the DON pool and an important source of biolability (Fellman et al., 2010; Lønborg et al., 2015; Yamashita et al., 2015). The inverse correlations between protein-like fluorescence and N/C ratios across seasons and sampling depths (Figure 3) suggest that proteins are generally not a major component of DON in BMF. We also observe only tentative evidence for protein consumption where surface layer tryptophan-like

**TABLE 4** | Annual freshwater and organic carbon (OC) fluxes from the four principal rivers entering Baker-Martinez Fjord.

	Baker	Pascua	Bravo	Huemules	Total
<b>Catchment properties<sup>a</sup></b>					
Total area (km <sup>2</sup> )	29,107	15,079	1,062	671	45,919
Glacial cover (%)	8	19	15	71	–
Forest cover (%)	20	12	23	4	–
Wetland cover excluding lakes (%)	4	4	4	4	–
Total lake volume ( $\times 10^6$ m <sup>3</sup> )	754,002	79,782	67	1,355	–
<b>Discharge<sup>b</sup></b>					
Mean summer (m <sup>3</sup> s <sup>-1</sup> )	1,268	835	–	218	–
Mean winter (m <sup>3</sup> s <sup>-1</sup> )	754	617	–	51	–
Mean annual (m <sup>3</sup> s <sup>-1</sup> )	932	714	112	121	–
Cumulative annual (km <sup>3</sup> a <sup>-1</sup> )	29.4	22.5	3.5	3.8	59.2
Share of annual freshwater input (%)	50	38	6	6	–
<b>Concentration data<sup>c</sup></b>					
SSC summer (mg L <sup>-1</sup> )	60.2	35.7	18.1	87.5	–
Sediment OC content (%)	0.19	0.38	0.25	0.09	–
POC summer (mg C L <sup>-1</sup> )	0.114	0.136	0.045	0.079	–
DOC summer (mg C L <sup>-1</sup> )	0.644	0.454	2.518	0.153	–
DOC winter (mg C L <sup>-1</sup> )	0.643	0.273	1.997	0.236	–
DOC annual mean (mg C L <sup>-1</sup> )	0.644	0.364	2.258	0.171	–
<b>Annual fluxes</b>					
SSC (Gg a <sup>-1</sup> )	1,769	804	64	334	2,971
POC (Mg C a <sup>-1</sup> )	3,360	3,056	160	301	6,877
DOC (Mg C a <sup>-1</sup> )	18,920	8,201	7,975	653	35,749
<b>TOTAL OC flux (Mg C a<sup>-1</sup>)</b>	<b>22,280</b>	<b>11,257</b>	<b>8,135</b>	<b>954</b>	<b>42,626</b>
POC (%)	15	27	2	32	16
DOC (%)	85	73	98	68	84
Share of annual OC input by rivers (%)	52	26	19	2	100

<sup>a</sup>Catchment areas calculated from a high resolution digital elevation model (Farr et al., 2007) using the Whitebox-GAT geospatial processing package (Lindsay, 2016). Catchment properties calculated from superimposed datasets including the Randolph Glacier Inventory (RGI Consortium, 2017), the National Mapping Organization's Global Land Cover raster (Tateishi et al., 2014), the SWAMP raster (Gumbrecht et al., 2019) and the HydroLAKES database (Messager et al., 2016).

<sup>b</sup>Discharge data sources as described in main text (Section "Flux Calculations").

<sup>c</sup>SSC and POC concentrations measured in summer only ( $n = 1$  for Baker, Pascua and Bravo;  $n = 25$  for Huemules). DOC concentrations measured in both summer ( $n = 1$  for Baker, Pascua and Bravo;  $n = 46$  for Huemules) and winter ( $n = 1$  for Baker, Pascua and Bravo;  $n = 15$  for Huemules). Concentrations expressed in units of mass per liter rather than molar units (used elsewhere) as more appropriate for flux calculations.

(C<sub>354</sub>) fluorescence falls to zero (**Supplementary Figure 3**) but this is not detectable in the molecular formulae associated with C<sub>354</sub> (**Figure 4G**). Moreover, consumption effects may be masked by autochthonous production in the fjord (**Supplementary Figure 3**).

## Changes in DOM Composition Along the Salinity Gradient

We use a correlative approach to track changes in DOM composition with salinity, similar to other coastal studies (Osterholz et al., 2016; Seidel et al., 2017). However, we are unable to assess mixing processes along a single axial transect as our samples are dispersed across a complex fjord system, capturing freshwater influences from multiple rivers and the Jorge Montt Glacier and marine water influences from two discrete entry routes at the mouths of the Baker and Martinez channels. These multiple end-members confound simple mixing analyses (Asmala et al., 2016). Instead, we interpret changes in DOM composition along a salinity gradient

that cuts across spatial, seasonal and depth variations, which reflect the overall shifting balance of marine and freshwater influences in the fjord.

The overall transition in the BMF from aromatic-rich DOM at low salinity to more saturated DOM at higher salinity (**Figure 4**) is typical of estuarine systems (Medeiros et al., 2015; Osterholz et al., 2016; Seidel et al., 2017). This is consistent with freshwater inputs from rivers as the major source of aromatic compounds (i.e., PPs and CAs) derived from degraded and leached vascular plants and soils (Ohno et al., 2010). The strong correlation between HUPs, especially N-HUPs, and salinity (**Figures 4C,D**) supports marine waters as a source of unsaturated and heteroatom-rich DOM (Medeiros et al., 2015; Osterholz et al., 2016). The similar trend for the 'island of stability' group (**Figure 4H**), a pool of stable molecular formulae that persist in the deep ocean (Lechtenfeld et al., 2014), suggests that subsurface waters in the BMF are likely to be a key source of these compounds and HUPs.

There is, however, considerable variability in the molecular composition of low salinity samples (**Figures 4E,F**), which makes

it difficult to reliably determine any non-conservative mixing patterns. For example, elevated relative intensities of PPs and CAs in the fjord surface layer with respect to some river samples (Figures 4E,F) could indicate substantial contributions of aromatic DOM from smaller streams and diffuse overland flow. However, the similar numbers of PP and CA formulae in rivers and fjord surface layer samples suggest that these downstream changes in relative intensity could just reflect an adjustment in internal composition as other DOM is added and other components possibly removed within the fjord.

The changes in molecular composition with salinity in BMF are consistent with the overall removal of aromatic DOM from surface waters by adsorption and flocculation processes (Sholkovitz, 1976). Photochemical degradation can also remove a wide range of compounds (HUPs, PPs, CAs) from surface waters (Spencer et al., 2009; Stubbins et al., 2010) but these processes will be limited by turbid conditions in BMF (Aracena et al., 2011; Marín et al., 2013). Bacterial degradation is also an effective removal mechanism for a wide range of phenolic and aromatic compounds (Stubbins et al., 2010; Medeiros et al., 2015; Mostovaya et al., 2017). Such processes might degrade terrestrial organic material and reinforce the inverse correlation between humic-like fluorescence and salinity (Figure 3). Alternatively, some bacteria might also convert reactive humic substances into more stable compounds (Shimotori et al., 2010; Romera-Castillo et al., 2011).

Trends in molecular composition with salinity do not necessarily capture changes in all DOM fractions. We speculate that complex patterns in protein-like fluorescence (Figure 3) arise from multiple sources and possible consumption processes affecting a small but reactive DOM fraction (Paulsen et al., 2018). Spikes in protein-like fluorescence (especially tryptophan-like, C<sub>354</sub>) in winter suggest a possible contribution from by-products of primary production (Murphy et al., 2008; Romera-Castillo et al., 2010; Lønborg et al., 2015), facilitated by reduced turbidity and less light limitation in the fjord. However, rapid utilization of autochthonous proteins by bacteria could maintain low protein-like fluorescence intensities at the surface in winter (Determann et al., 1998; Yamashita et al., 2008). Moderate protein-like fluorescence in some subsurface samples suggests that sinking organic matter may undergo bacterial degradation or sloppy feeding by grazers (Poulet et al., 1991; Urban-Rich et al., 2004; Møller, 2007). Higher subsurface protein-like fluorescence in summer could indicate that large seasonal inputs of terrestrial organic matter are processed by fjord ecosystems (Meerhoff et al., 2019) and undergo bacterial degradation at depth (Nagata et al., 2000; Fox et al., 2017).

## Assessing the Importance of Riverine OC Fluxes to Baker-Martinez Fjord

Due to scarcity in biogeochemical data from this region, our estimate of  $> 42 \text{ Gg C a}^{-1}$  is the first attempt to calculate the combined annual OC flux of the four main rivers draining into BMF (Table 4). This value likely underestimates the total flux into the BMF as we were unable to constrain inputs from the marine-terminating Jorge Montt Glacier. The estimate is also based on

a limited sample set but the data used in our calculations are broadly consistent with previously reported POC concentrations ( $0.074\text{--}0.158 \text{ mg C L}^{-1}$ ; Vargas et al., 2011), although there are no published DOC concentrations to compare to our measurements. Nevertheless, we contend that our calculations provide a useful, conservative baseline for monitoring future changes in OC export in response to upstream landscape change linked to glacier retreat (Milner et al., 2017).

Our OC flux estimate ( $\sim 40 \text{ Gg C a}^{-1}$ ) is relatively modest in global terms, even for glacially influenced regions. For example, the estimated annual export of carbon from the Greenland Ice Sheet is two orders of magnitude larger ( $\sim 1500 \text{ Gg C a}^{-1}$ ; Lawson et al., 2014; Hood et al., 2015) and those from the Himalayas ( $\sim 100 \text{ Gg C a}^{-1}$ ; Hemingway et al., 2019) and Gulf of Alaska ( $\sim 130 \text{ Gg C a}^{-1}$ ; Hood et al., 2009) are over twice the size. However, area-normalized fluxes (or yields) demonstrate that OC export from our study catchments is consistent with the range of estimates for other glaciated regions. We calculate a combined annual OC yield of  $0.93 \text{ Mg C km}^{-2} \text{ a}^{-1}$  for the four main river basins draining into the BMF, assuming a combined catchment area of  $\sim 46 \times 10^3 \text{ km}^2$ . This compares with an estimated yield for the Greenland Ice Sheet of  $0.88 \text{ Mg C km}^{-2} \text{ a}^{-1}$ , assuming an area of  $\sim 1,700 \times 10^3 \text{ km}^2$  (Hawkings et al., 2016), and lies within the range of reported yields for the Himalayas,  $0.50 \text{ Mg C km}^{-2} \text{ a}^{-1}$  (Hemingway et al., 2019), and the Gulf of Alaska,  $1.65 \text{ Mg C km}^{-2} \text{ a}^{-1}$  (Hood et al., 2009).

Comparing our riverine OC flux to crude estimates of carbon fixation by primary production suggests that rivers supply a substantial proportion (10–64%) of the total annual OC input to BMF (Supplementary Table 2). Even the lower range of our estimates (10%) supports rivers being an important source of carbon to the fjord heads, where primary production is most limited (Vargas et al., 2011; González et al., 2013). In general, primary production rates are lower in BMF than in other Chilean fjords with weaker glacial influences (Aracena et al., 2011) but spatiotemporal variabilities make it difficult to constrain annual carbon fixation across the fjord (Supplementary Table 2). Overall, we regard our calculations as conservative in favor of autochthonous production due to the use of springtime primary production rates, which reflect peak productivity (Aracena et al., 2011; González et al., 2013; Jacob et al., 2014), and an underestimation of allochthonous inputs. For example, freshwater fluxes from Jorge Montt Glacier are substantial ( $1.9\text{--}4.5 \text{ km}^3 \text{ a}^{-1}$ , 2012–2017; Bown et al., 2019) but we cannot constrain OC export from this glacier as the OC concentration of its meltwaters is unknown.

The bulk composition of riverine OC shows a dominance of DOC over POC that is in line with the broad range of conditions in fjords across Chilean Patagonia and the Arctic (Table 5) but is atypical of glacial rivers where POC may comprise 50–90% of the total OC load (Lawson et al., 2014; Hood et al., 2015). This suggests that proglacial lakes are a major upstream sink for particulates, including biolabile POC (Meyers et al., 1984; Carrivick and Tweed, 2013). Although SSCs are low ( $< 0.1 \text{ g L}^{-1}$ ) compared to typical glacial rivers ( $0.5\text{--}10 \text{ g L}^{-1}$ ) (Knudsen et al., 2007; Lawson et al., 2014), we

**TABLE 5** | Dissolved organic carbon: POC ratios for major input rivers of the Baker-Martinez Fjord compared to published data for water masses in other fjords and channels in Chilean Patagonia and the Arctic.

Location and sample	Sample type	DOC (mg L <sup>-1</sup> )	POC (mg L <sup>-1</sup> )	DOC:POC	Study
CHILEAN PATAGONIA					
<i>Baker-Martinez Fjord</i>					
Baker River <sup>a</sup>	River	0.644	0.114	5.6	<i>This study</i>
Pascua River <sup>a</sup>	River	0.364	0.136	2.7	<i>This study</i>
Huemules River <sup>a</sup>	River	0.153	0.079	1.9	<i>This study</i>
Bravo River <sup>a</sup>	River	2.518	0.045	56.0	<i>This study</i>
Martinez Channel <sup>b</sup>	Surface fjord	1.320	0.140	9.4	1
<i>Inner Sea of Chiloé</i>					
Mean for inner sea area <sup>b</sup>	Surface marine	0.910	0.256	3.6	2
Reloncavi Fjord <sup>c</sup>	Surface fjord	0.740	0.325	2.3	2
<i>Magellan Strait</i>					
Magellan Strait <sup>b</sup>	Surface marine	1.720	0.392	4.4	3
Beagle Magellan Water	Subsurface marine	0.815	0.234	3.5	4
Sub-Antarctic Shelf Water	Subsurface marine	0.700	0.129	5.4	4
Sub-Antarctic Water	Subsurface marine	0.640	0.077	8.3	4
ARCTIC					
<i>Young Sound, Greenland<sup>d</sup></i>					
	Surface fjord	1.285	0.024	53.5	5
	Subsurface fjord	1.261	0.026	48.5	5
	Shelf water	1.068	0.025	42.7	5
	River	0.504	0.056	9.0	5
<i>Kongsfjorden, Svalbard</i>					
October	Surface fjord	1.158	0.189	6.1	6
April	Surface fjord	0.713	0.283	2.5	6
August	Surface fjord	1.091	0.276	4.0	7
August	Subsurface fjord	1.309	0.068	19.3	7
August	River	0.877	0.673	1.3	7
<i>Norway</i>					
Ballsfjord	Surface fjord	1.500	0.748	2.0	8
Ullsfjord	Surface fjord	1.370	0.325	4.2	8

<sup>a</sup>Annual mean concentrations reported in **Table 4**.

<sup>b</sup>DOC:POC calculated from concentrations converted from depth-integrated concentrations reported in study.

<sup>c</sup>As *b*. but concentrations read off from graph in study and expressed as mean for all stations within Reloncavi Fjord.

<sup>d</sup>Mean concentrations for summer (July) study period; molar DOC concentrations converted into mg L<sup>-1</sup>.

(1) González et al., 2013; (2) González et al., 2019; (3) González et al., 2016; (4) Barrera et al., 2017; (5) Paulsen et al., 2017; (6) Brogi et al., 2019; (7) Zhu et al., 2016; (8) Gašparović et al., 2005.

may overestimate annual POC fluxes by using summer SSCs, which can be double winter values in the Baker River (Quiroga et al., 2012). Our results therefore provide a conservative estimate for the importance of riverine DOC as a carbon subsidy to the fjord.

Bulk composition is an important factor affecting the fate of riverine OC in BMF. Strong inputs of terrestrial POC drive high rates of carbon burial at the fjord heads (Rebolledo et al., 2019) and supplement available food sources for zooplankton (Meerhoff et al., 2019). However, the larger and more biolabile DOC flux is likely to be critical for bacterial carbon cycling in the fjord (Vargas et al., 2011; Brett et al., 2017). Riverine DOC may be especially important for bacteria in the near-shore zone in summer (González et al., 2013), when discharge is highest and autochthonous substrates are lacking (Aracena et al., 2011). We would therefore expect carbon cycling in BMF to be sensitive to changes in the supply of biolabile OC from rivers as a result of accelerated glacier melting and retreat (Foresta et al., 2018).

## Biogeochemical Impacts of Changing Glacier Melt Inputs on Baker-Martinez Fjord

Seasonal and spatial variation in DOM composition, coupled to the relative importance of riverine OC inputs, suggest that glaciers exert an important control over the biogeochemistry of BMF. We hypothesize the following biogeochemical impacts of enhanced glacier melting on BMF, which highlight potential sensitivities in other glaciated fjords, especially those in wet maritime regions.

### 1. Reduced efficiency of the fjord as a carbon sink.

The strongest molecular signatures of recent primary production in BMF occur in the surface layer DOM pool in winter (**Figure 6**). This is consistent with strong turbid meltwater inputs in summer suppressing the fixation of new carbon by primary production. In the short-term, these effects could intensify through enhanced melting

of the NPI and SPI and the production of deeper and longer lasting turbid meltwater plumes (Foresta et al., 2018). Higher sedimentation rates and the binding of organic matter to sediment surfaces (Sholkovitz, 1976) could increase carbon burial efficiency in inner fjord areas but these processes are likely to be dominated by older, terrestrial carbon sources (Rebolledo et al., 2019). Although fjords are globally important carbon sinks (Smith et al., 2015), the probable decline in fjord primary production (Aracena et al., 2011; Włodarska-Kowalczyk et al., 2019) may mean that Patagonian fjords play a reduced role in new carbon sequestration.

2. **Carbon cycling will be increasingly influenced by allochthonous DOM.** The sensitivity of surface layer DOM composition to changes in river inputs, coupled to the widespread and year-round presence of aromatic and humic-rich DOM reported here shows that terrestrial inputs are a significant source of organic matter for the ecosystem in BMF. In the short term, allochthonous DOM from enhanced meltwater discharge may become an increasingly important resource for heterotrophic bacteria in the fjord (González et al., 2013), especially if inputs of glacial DOM are highly labile (Hood et al., 2009; Fellman et al., 2010). In the long term, glacier retreat may lead to reduced DOC export in summer and allow rain-driven export of aromatic and humic-rich DOM from soils and wetlands in winter to dominate annual fluxes (Fellman et al., 2010; Milner et al., 2017). In the absence of more readily labile material, these terrestrial DOM sources could become the most important substrate for fjord bacteria (Mostovaya et al., 2017).
- 3 **Changes in organic nitrogen substrates available to fjord communities.** Seasonal changes in peptide-like formulae in the BMF (Figure 5 and Table 3) suggest that the composition of biolabile components of the DON pool are sensitive to changes in the strength of freshwater (and hence meltwater) inputs. Changes in water and DON supply could affect plankton community structure and nitrogen cycling processes, given the selective consumption of biolabile N-compounds by phytoplankton and heterotrophic bacteria (Liu et al., 2017). This may have particular relevance where DON is an important source of biolabile N for planktonic communities in N-limited fjords (Bronk et al., 2007; González et al., 2011; Iriarte et al., 2014).
- 4 **Expansion of the above conditions as marine-terminating glaciers retreat onto land.** The limited observational data from Jorge Montt Fjord suggest that conditions in this inlet differ slightly from the rest of BMF, with higher surface DON in summer accompanied by lower turbidity and higher chlorophyll levels (Table 1). However, the rapid, ongoing retreat of Jorge Montt Glacier may eventually produce a new land-terminating glacier and redirect the present submarine discharge of meltwaters to the surface layer (Rivera et al., 2012). This will likely lead to reduced downstream primary productivity as turbidity

levels in this sector of the fjord become more similar to those in Steffen Fjord and the heads of the Baker and Martinez channels. Such hypothesized changes are also applicable to the fjords on the western side of the SPI where other marine-terminating glaciers are retreating (Foresta et al., 2018).

## CONCLUSION

We have presented the first detailed analysis of DOM composition in a Chilean Patagonian fjord, using molecular level techniques that have improved understanding of DOM cycling in other aquatic environments. Our results suggest that significant seasonal differences in DOM composition in the surface waters of BMF are controlled by variations in river discharge linked to glacier melt cycles. The changes in fjord surface layer DOM may reflect a combination of seasonal changes in riverine DOM composition, differences in the degree of mixing of subsurface and surface DOM sources, and the regulation of primary production and new DOM formation by turbid river plumes. The composition of peptide-like formulae in the surface waters may be particularly sensitive to these seasonal controls on DOM composition, with implications for the cycling of biolabile DON. Trends in DOM composition with increasing salinity observed here are typical of estuarine systems and suggest preferential removal of terrestrial aromatic compounds and increased influence of unsaturated and heteroatom-rich compounds from marine sources. Our results also demonstrate that glacially fed rivers could provide a major supply of DOC to the BMF and influence carbon cycling processes. Overall, these findings indicate that the composition and processing of DOM in BMF will be affected by the accelerated melting of the NPI and SPI, which suggests biogeochemical sensitivity for other glaciated fjords in a warming climate.

## DATA AVAILABILITY STATEMENT

Publicly available datasets were analyzed in this study. This data can be found here: <https://zenodo.org/record/4603220#.YEz-EOj7SUK>.

## AUTHOR CONTRIBUTIONS

MM and AK developed the study from the aims of the NERC/CONICYT-funded PISCES research project, which was conceived by JW and LR. MM conducted all analyses with significant assistance from AK in FT-ICR MS analysis and JH in macronutrient analyses. MM wrote the manuscript, with contributions from AK, JW, JH, and RS. All authors contributed to fieldwork operations and data collection.

## FUNDING

This work was part of the NERC/CONICYT-funded PISCES project (NE/P003133/1 – PII20150106). MM was funded by a

Ph.D. studentship through the NERC GW4+ Doctoral Training Partnership (NE/L002434/1). The National High Magnetic Field Laboratory, Tallahassee, FL, United States, provided instrument time and a travel bursary to MM to conduct FT-ICR MS analysis. JH was supported by a European Commission Horizon 2020 Marie Skłodowska-Curie Actions fellowship ICICLES (Grant Agreement #793962). JW also acknowledges a Royal Society Wolfson Merit Award and a Leverhulme Trust Senior Research Fellowship.

## ACKNOWLEDGMENTS

We sincerely thank everyone who assisted with fieldwork in Chile, including the crew of the *R.V. Sur Austral* (COPAS, Tortel, Chile), the team at the Centro de Investigación en Ecosistemas

de la Patagonia (CIEP, Coyhaique, Chile), and Dr. Sebastien Bertrand and team (University of Ghent, Belgium). Special thanks to Dr. Kate Hendry (co-investigator on PISCES project, University of Bristol) for assistance in boat survey planning. We wish to thank the National High Magnetic Field Laboratory, Tallahassee, FL, United States, for providing instrument time and Dr. Lissa Anderson, in particular, for technical support. We thank Dr. Fotis Sgouridis and James Williams for laboratory support at LOWTEX (University of Bristol, United Kingdom).

## SUPPLEMENTARY MATERIAL

The Supplementary Material for this article can be found online at: <https://www.frontiersin.org/articles/10.3389/fmars.2021.612386/full#supplementary-material>

## REFERENCES

- Aiken, C. M. (2012). Seasonal thermal structure and exchange in Baker Channel, Chile. *Dyn. Atmos. Oceans* 58, 1–19. doi: 10.1016/j.dynatmoce.2012.07.001
- Aluwihare, L. I., and Meador, T. (2008). “Chemical composition of marine dissolved organic nitrogen,” in *Nitrogen in the Marine Environment*, eds D. G. Capone, D. A. Bronk, M. R. Mulholland, and E. J. Carpenter (Cambridge, MA: Academic Press). doi: 10.1016/B978-0-12-372522-6.00003-7
- Aluwihare, L. I., Repeta, D. J., Pantoja, S., and Johnson, C. G. (2005). Two chemically distinct pools of organic nitrogen accumulate in the ocean. *Science* 308, 1007–1010. doi: 10.1126/science.1108925
- Amon, R. M. W., and Benner, R. (1994). Rapid cycling of high-molecular-weight dissolved organic matter in the ocean. *Nature* 369, 549–552. doi: 10.1038/369549a0
- Aracena, C., Kilian, R., Lange, C. B., Bertrand, S., Lamy, F., Arz, H. W., et al. (2015). Holocene variations in productivity associated with changes in glacier activity and freshwater flux in the central basin of the Strait of Magellan. *Palaeogeogr. Palaeoclimatol. Palaeoecol.* 436, 112–122. doi: 10.1016/j.palaeo.2015.06.023
- Aracena, C., Lange, C. B., Rebolledo, L., Iriarte, J. L., Rebolledo, L., and Pantoja, S. (2011). Latitudinal patterns of export production recorded in surface sediments of the Chilean Patagonian fjords (41–55°S) as a response to water column productivity. *Continental Shelf Res.* 31, 340–355. doi: 10.1016/j.csr.2010.08.008
- Armbruster, D. A., and Pry, T. (2008). Limit of blank, limit of detection and limit of quantitation. *Clin. Biochem. Rev.* 29(Suppl. 1), S49–S52.
- Asmala, E., Kaartokallio, H., Carstensen, J., and Thomas, D. N. (2016). Variation in riverine inputs affect dissolved organic matter characteristics throughout the estuarine gradient. *Front. Mar. Sci.* 2:125. doi: 10.3389/fmars.2015.00125
- Aufdenkampe, A. K., Hedges, J. I., Richey, J. E., Krusche, A. V., and Llerena, C. A. (2001). Sorptive fractionation of dissolved organic nitrogen and amino acids onto fine sediments within the Amazon Basin. *Limnol. Oceanogr.* 46, 1921–1935. doi: 10.4319/lo.2001.46.8.1921
- Barker, J. D., Sharp, M. J., Fitzsimons, S. J., and Turner, R. J. (2006). Abundance and dynamics of dissolved organic carbon in glacier systems. *Arctic Antarctic Alpine Res.* 38, 163–172.
- Barrera, F., Lara, R. J., Krock, B., Garzón-Cardona, J. E., Fabro, E., and Koch, B. P. (2017). Factors influencing the characteristics and distribution of surface organic matter in the Pacific-Atlantic connection. *J. Mar. Syst.* 175, 36–45. doi: 10.1016/j.jmarsys.2017.07.004
- Bartholomew, I., Nienow, P., Sole, A., Mair, D., Cowton, T., Palmer, S., et al. (2011). Supraglacial forcing of subglacial drainage in the ablation zone of the Greenland ice sheet. *Geophys. Res. Lett.* 38:L08502. doi: 10.1029/2011GL047063
- Benjamini, Y., and Hochberg, Y. (1995). Controlling the false discovery rate: A practical and powerful approach to multiple testing. *J. R. Stat. Soc. Ser. B (Methodological)* 57, 289–300. doi: 10.1111/j.2517-6161.1995.tb02031.x
- Bianchi, T. S., Arndt, S., Austin, W. E. N., Benn, D. I., Bertrand, S., Cui, X., et al. (2020). Fjords as Aquatic Critical Zones (ACZs). *Earth Sci. Rev.* 203:103145. doi: 10.1016/j.earscirev.2020.103145
- Bown, F., Rivera, A., Pętllicki, M., Bravo, C., Oberreuter, J., and Moffat, C. (2019). Recent ice dynamics and mass balance of Jorge Montt Glacier, Southern Patagonia Icefield. *J. Glaciol.* 65, 732–744. doi: 10.1017/jog.2019.47
- Brett, M. T., Bunn, S. E., Chandra, S., Galloway, A. W. E., Guo, F., Kainz, M. J., et al. (2017). How important are terrestrial organic carbon inputs for secondary production in freshwater ecosystems? *Freshw. Biol.* 62, 833–853. doi: 10.1111/fwb.12909
- Broggi, S. R., Jung, J. Y., Ha, S. Y., and Hur, J. (2019). Seasonal differences in dissolved organic matter properties and sources in an Arctic fjord: implications for future conditions. *Sci. Total Environ.* 694:133740. doi: 10.1016/j.scitotenv.2019.133740
- Bronk, D. A., See, J. H., Bradley, P., and Killberg, L. (2007). DON as a source of bioavailable nitrogen for phytoplankton. *Biogeosciences* 4, 283–296. doi: 10.5194/bg-4-283-2007
- Burd, A. B., Frey, S., Cabre, A., Ito, T., Levine, N. M., Lønborg, C., et al. (2016). Terrestrial and marine perspectives on modeling organic matter degradation pathways. *Glob. Change Biol.* 22, 121–136. doi: 10.1111/gcb.12987
- Carrivick, J. L., and Tweed, F. S. (2013). Proglacial lakes: character, behaviour and geological importance. *Quaternary Sci. Rev.* 78, 34–52. doi: 10.1016/j.quascirev.2013.07.028
- Cuevas, L. A., Tapia, F. J., Iriarte, J. L., González, H. E., Silva, N., and Vargas, C. A. (2019). Interplay between freshwater discharge and oceanic waters modulates phytoplankton size-structure in fjords and channel systems of the Chilean Patagonia. *Prog. Oceanogr.* 173, 103–113. doi: 10.1016/j.pocean.2019.02.012
- Determann, S., Lobbes, J. M., Reuter, R., and Rullkötter, J. (1998). Ultraviolet fluorescence excitation and emission spectroscopy of marine algae and bacteria. *Mar. Chem.* 62, 137–156. doi: 10.1016/S0304-4203(98)00026-7
- Dirección General de Aguas (2019). *Hydrometeorological Service: DGA Stations Statistics*. Santiago, CA: Dirección General de Aguas.
- Dittmar, T., Koch, B., Hertkorn, N., and Kattner, G. (2008). A simple and efficient method for the solid-phase extraction of dissolved organic matter (SPE-DOM) from seawater. *Limnol. Oceanogr. Methods* 6, 230–235. doi: 10.4319/lom.2008.6.230
- Dubnick, A., Barker, J., Sharp, M., Wadham, J., Lis, G., Telling, J., et al. (2010). Characterization of dissolved organic matter (DOM) from glacial environments using total fluorescence spectroscopy and parallel factor analysis. *Anal. Glaciol.* 51, 111–122.
- Dussaillant, A. J., Buytaert, W., Meier, C., and Espinoza, F. (2012). Hydrological regime of remote catchments with extreme gradients under accelerated change: the Baker basin in Patagonia. *Hydrol. Sci. J.* 57, 1530–1542. doi: 10.1080/02626667.2012.726993
- Dussaillant, I., Berthier, E., Brun, F., Masiokas, M., Hugonnet, R., Favier, V., et al. (2019). Two decades of glacier mass loss along the Andes. *Nat. Geosci.* 12, 802–808. doi: 10.1038/s41561-019-0432-5
- Eisma, D. (1986). Flocculation and de-flocculation of suspended matter in estuaries. *Netherlands J. Sea Res.* 20, 183–199. doi: 10.1016/0077-7579(86)90041-4

- Farr, T. G., Rosen, P. A., Caro, E., Crippen, R., Duren, R., Hensley, S., et al. (2007). The shuttle radar topography mission. *Rev. Geophys.* 45:RG2004. doi: 10.1029/2005RG000183
- Fellman, J. B., D'Amore, D. V., Hood, E., and Boone, R. D. (2008). Fluorescence characteristics and biodegradability of dissolved organic matter in forest and wetland soils from coastal temperate watersheds in southeast Alaska. *Biogeochemistry* 88, 169–184. doi: 10.1007/s10533-008-9203-x
- Fellman, J. B., Hood, E., Raymond, P. A., Hudson, J., Bozeman, M., and Arimitsu, M. (2015). Evidence for the assimilation of ancient glacier organic carbon in a proglacial stream food web. *Limnol. Oceanogr.* 60, 1118–1128. doi: 10.1002/lno.10088
- Fellman, J. B., Hood, E., Spencer, R. G. M., Stubbins, A., and Raymond, P. A. (2014). Watershed glacier coverage influences dissolved organic matter biogeochemistry in coastal watersheds of southeast Alaska. *Ecosystems* 17, 1014–1025. doi: 10.1007/s10021-014-9777-1
- Fellman, J. B., Spencer, R. G. M., Hernes, P. J., Edwards, R. T., D'Amore, D. V., and Hood, E. (2010). The impact of glacier runoff on the biodegradability and biochemical composition of terrigenous dissolved organic matter in near-shore marine ecosystems. *Mar. Chem.* 121, 112–122. doi: 10.1016/j.marchem.2010.03.009
- Foresta, L., Gourmelen, N., Weissgerber, F., Nienow, P., Williams, J. J., Shepherd, A., et al. (2018). Heterogeneous and rapid ice loss over the Patagonian Ice Fields revealed by CryoSat-2 swath radar altimetry. *Remote Sensing Environ.* 211, 441–455. doi: 10.1016/j.rse.2018.03.041
- Fox, B. G., Thorn, R. M. S., Anesio, A. M., and Reynolds, D. M. (2017). The in situ bacterial production of fluorescent organic matter: an investigation at a species level. *Water Res.* 125, 350–359. doi: 10.1016/j.watres.2017.08.040
- Gasparović, B., Plavšić, M., Čosović, B., and Reigstad, M. (2005). Organic matter characterization and fate in the sub-arctic Norwegian fjords during the late spring/summer period. *Estuarine Coastal Shelf Sci.* 62, 95–107. doi: 10.1016/j.ecss.2004.08.008
- Glasser, N. F., Harrison, S., Jansson, K. N., Anderson, K., and Cowley, A. (2011). Global sea-level contribution from the Patagonian Icefields since the Little Ice Age maximum. *Nat. Geosci.* 4, 303–307. doi: 10.1038/ngeo1122
- González, H. E., Castro, L., Daneri, G., Iriarte, J. L., Silva, N., Vargas, C. A., et al. (2011). Seasonal plankton variability in Chilean Patagonia fjords: carbon flow through the pelagic food web of Aysen Fjord and plankton dynamics in the Moraleda Channel basin. *Continental Shelf Res.* 31, 225–243. doi: 10.1016/j.csr.2010.08.010
- González, H. E., Castro, L. R., Daneri, G., Iriarte, J. L., Silva, N., Tapia, F., et al. (2013). Land–ocean gradient in haline stratification and its effects on plankton dynamics and trophic carbon fluxes in Chilean Patagonian fjords (47–50°S). *Prog. Oceanogr.* 119, 32–47. doi: 10.1016/j.poc.2013.06.003
- González, H. E., Graeve, M., Kattner, G., Silva, N., Castro, L., Iriarte, J. L., et al. (2016). Carbon flow through the pelagic food web in southern Chilean Patagonia: Relevance of Euphausia vallentini as a key species. *Mar. Ecol. Prog. Ser.* 557, 91–110. doi: 10.3354/meps11826
- González, H. E., Nimptsch, J., Giesecke, R., and Silva, N. (2019). Organic matter distribution, composition and its possible fate in the Chilean North-Patagonian estuarine system. *Sci. Total Environ.* 657, 1419–1431. doi: 10.1016/j.scitotenv.2018.11.445
- Gumbricht, T., Román-Cuesta, R. M., Verchot, L. V., Herold, M., Wittmann, F., Householder, E., et al. (2019). *Tropical and Subtropical Wetlands Distribution Version 2*. Bogor: Center for International Forestry Research. doi: 10.17528/CIFOR/DATA.00058
- Gutiérrez, M. H., Galand, P. E., Moffat, C., and Pantoja, S. (2015). Melting glacier impacts community structure of Bacteria, Archaea and Fungi in a Chilean Patagonia fjord. *Environ. Microbiol.* 17, 3882–3897. doi: 10.1111/1462-2920.12872
- Hågvær, S., and Ohlson, M. (2013). Ancient carbon from a melting glacier gives high <sup>14</sup>C age in living pioneer invertebrates. *Sci. Rep.* 3:2820. doi: 10.1038/srep02820
- Hawkings, J., Wadham, J., Tranter, M., Telling, J., Bagshaw, E., Beaton, A., et al. (2016). The Greenland Ice Sheet as a hot spot of phosphorus weathering and export in the Arctic. *Glob. Biogeochem. Cycles* 30, 191–210. doi: 10.1002/2015GB005237
- Hawkings, J. R., Wadham, J. L., Tranter, M., Lawson, E., Sole, A., Cowton, T., et al. (2015). The effect of warming climate on nutrient and solute export from the Greenland Ice Sheet. *Geochem. Perspect. Lett.* 1, 94–104. doi: 10.7185/geochemlet.1510
- Hawkings, J. R., Wadham, J. L., Tranter, M., Raiswell, R., Benning, L. G., Statham, P. J., et al. (2014). Ice sheets as a significant source of highly reactive nanoparticulate iron to the oceans. *Nat. Commun.* 5:3929. doi: 10.1038/ncomms4929
- Hedges, J. I., and Stern, J. H. (1984). Carbon and nitrogen determinations of carbonate-containing solids. *Limnol. Oceanogr.* 29, 657–663. doi: 10.4319/lno.1984.29.3.0657
- Hemingway, J. D., Spencer, R. G. M., Podgorski, D. C., Zito, P., Sen, I. S., and Galy, V. V. (2019). Glacier meltwater and monsoon precipitation drive Upper Ganges Basin dissolved organic matter composition. *Geochim. Cosmochim. Acta* 244, 216–228. doi: 10.1016/j.gca.2018.10.012
- Hernes, P. J., and Benner, R. (2003). Photochemical and microbial degradation of dissolved lignin phenols: implications for the fate of terrigenous dissolved organic matter in marine environments. *J. Geophys. Res. C Oceans* 108:3291.
- Hood, E., Battin, T. J., Fellman, J., Neel, S. O., Spencer, R. G. M., O'Neil, S., et al. (2015). Storage and release of organic carbon from glaciers and ice sheets. *Nat. Geosci.* 8, 91–96. doi: 10.1038/ngeo2331
- Hood, E., Fellman, J., Spencer, R. G. M., Hernes, P. J., Edwards, R., D'Amore, D., et al. (2009). Glaciers as a source of ancient and labile organic matter to the marine environment. *Nature* 462, 1044–1047. doi: 10.1038/nature08580
- Hopkinson, C. S., Buffam, I., Hobbie, J., Vallino, J., Perdue, M., Eversmeyer, B., et al. (1998). Terrestrial inputs of organic matter to coastal ecosystems: an intercomparison of chemical characteristics and bioavailability. *Biogeochemistry* 43, 211–234. doi: 10.1023/A:1006016030299
- Hopwood, M. J., Carroll, D., Browning, T. J., Meire, L., Mortensen, J., Krisch, S., et al. (2018). Non-linear response of summertime marine productivity to increased meltwater discharge around Greenland. *Nat. Commun.* 9:3256. doi: 10.1038/s41467-018-05488-8
- Hopwood, M. J., Carroll, D., Dunse, T., Hodson, A., Holding, J. M., Iriarte, J. L., et al. (2020). Review article: how does glacier discharge affect marine biogeochemistry and primary production in the Arctic? *Cryosphere* 14, 1347–1383. doi: 10.5194/tc-14-1347-2020
- Hosomi, M., and Sudo, R. (1986). Simultaneous determination of total nitrogen and total phosphorus in freshwater samples using persulfate digestion. *Int. J. Environ. Stud.* 27, 267–275. doi: 10.1080/00207238608710296
- Iriarte, J. L., González, H. E., Liu, K. K., Rivas, C., and Valenzuela, C. (2007). Spatial and temporal variability of chlorophyll and primary productivity in surface waters of southern Chile (41.5–43° S). *Estuarine Coastal Shelf Sci.* 74, 471–480. doi: 10.1016/j.ecss.2007.05.015
- Iriarte, J. L., Pantoja, S., and Daneri, G. (2014). Oceanographic processes in Chilean fjords of Patagonia: from small to large-scale studies. *Prog. Oceanogr.* 129, 1–7. doi: 10.1016/j.poc.2014.10.004
- Jacob, B. G., Tapia, F. J., Daneri, G., Iriarte, J. L., Montero, P., Sobarzo, M., et al. (2014). Springtime size-fractionated primary production across hydrographic and PAR-light gradients in Chilean Patagonia (41–50°S). *Prog. Oceanogr.* 129, 75–84. doi: 10.1016/j.poc.2014.08.003
- Keil, R. G., Montluçon, D. B., Prahl, F. G., and Hedges, J. I. (1994). Sorptive preservation of labile organic matter in marine sediments. *Nature* 370, 549–552. doi: 10.1038/370549a0
- Kellerman, A. M., Guillemette, F., Podgorski, D. C., Aiken, G. R., Butler, K. D., and Spencer, R. G. M. (2018). Unifying concepts linking dissolved organic matter composition to persistence in aquatic ecosystems. *Environ. Sci. Technol.* 52, 2538–2548. doi: 10.1021/acs.est.7b05513
- Kellerman, A. M., Hawkings, J. R., Wadham, J. L., Kohler, T. J., Stibal, M., Grater, E., et al. (2020). Glacier outflow dissolved organic matter as a window into seasonally changing carbon sources: Leverett Glacier, Greenland. *J. Geophys. Res. Biogeosci.* 125:e2019JG005161. doi: 10.1029/2019jg005161
- Knudsen, N. T., Yde, J. C., and Gasser, G. (2007). Suspended sediment transport in glacial meltwater during the initial quiescent phase after a major surge event at Kuannersuit Glacier, Greenland. *Geografisk Tidsskrift.* 107, 1–7. doi: 10.1080/00167223.2007.10801370

- Koch, B. P., and Dittmar, T. (2006). From mass to structure: an aromaticity index for high-resolution mass data of natural organic matter. *Rapid Commun. Mass Spectrom.* 20, 926–932. doi: 10.1002/rcm.2386
- Koch, B. P., Witt, M., Engbrodt, R., Dittmar, T., and Kattner, G. (2005). Molecular formulae of marine and terrigenous dissolved organic matter detected by electrospray ionization Fourier transform ion cyclotron resonance mass spectrometry. *Geochim. Cosmochim. Acta* 69, 3299–3308. doi: 10.1016/j.gca.2005.02.027
- Kujawinski, E. B., Longnecker, K., Blough, N. V., Vecchio, R., Del Finlay, L., Kitner, J. B., et al. (2009). Identification of possible source markers in marine dissolved organic matter using ultrahigh resolution mass spectrometry. *Geochim. Cosmochim. Acta* 73, 4384–4399. doi: 10.1016/j.gca.2009.04.033
- Landa, M., Cottrell, M. T., Kirchman, D. L., Kaiser, K., Medeiros, P. M., Tremblay, L., et al. (2014). Phylogenetic and structural response of heterotrophic bacteria to dissolved organic matter of different chemical composition in a continuous culture study. *Environ. Microbiol.* 16, 1668–1681. doi: 10.1111/1462-2920.12242
- Lawson, E. C., Wadham, J. L., Tranter, M., Stibal, M., Lis, G. P., Butler, C. E. H., et al. (2014). Greenland ice sheet exports labile organic carbon to the arctic oceans. *Biogeosciences* 11, 4015–4028. doi: 10.5194/bg-11-4015-2014
- Lechtenfeld, O. J., Kattner, G., Flerus, R., McCallister, S. L., Schmitt-Kopplin, P., and Koch, B. P. (2014). Molecular transformation and degradation of refractory dissolved organic matter in the Atlantic and Southern Ocean. *Geochim. Cosmochim. Acta* 126, 321–337. doi: 10.1016/j.gca.2013.11.009
- Lindsay, J. B. (2016). Whitebox GAT: a case study in geomorphometric analysis. *Comput. Geosci.* 95, 75–84. doi: 10.1016/j.cageo.2016.07.003
- Liu, S., Wawrik, B., and Liu, Z. (2017). Different bacterial communities involved in peptide decomposition between normoxic and hypoxic coastal waters. *Front. Microbiol.* 8:353. doi: 10.3389/fmicb.2017.00353
- Lønborg, C., Yokokawa, T., Herndl, G. J., and Antón Álvarez-Salgado, X. (2015). Production and degradation of fluorescent dissolved organic matter in surface waters of the eastern north Atlantic ocean. *Deep Sea Res. Part I Oceanogr. Res. Papers* 96, 28–37. doi: 10.1016/j.dsr.2014.11.001
- Marin, V. H., Tironi, A., Paredes, M. A., and Contreras, M. (2013). Modeling suspended solids in a Northern Chilean Patagonia glacier-fed fjord: GLOF scenarios under climate change conditions. *Ecol. Model.* 264, 7–16. doi: 10.1016/j.ecolmodel.2012.06.017
- Medeiros, P. M., Seidel, M., Ward, N. D., Carpenter, E. J., Gomes, H. R., Niggemann, J., et al. (2015). Fate of the Amazon River dissolved organic matter in the tropical Atlantic Ocean. *Glob. Biogeochem. Cycles* 29, 677–690. doi: 10.1002/2015GB005115
- Meerhoff, E., Castro, L. R., Tapia, F. J., and Pérez-Santos, I. (2019). Hydrographic and Biological Impacts of a Glacial Lake Outburst Flood (GLOF) in a Patagonian Fjord. *Estuaries Coasts* 42, 132–143. doi: 10.1007/s12237-018-0449-9
- Meire, L., Mortensen, J., Meire, P., Juul-Pedersen, T., Sejr, M. K., Rysgaard, S., et al. (2017). Marine-terminating glaciers sustain high productivity in Greenland fjords. *Glob. Change Biol.* 23, 5344–5357. doi: 10.1111/gcb.13801
- Messenger, M. L., Lehner, B., Grill, G., Nedeva, I., and Schmitt, O. (2016). Estimating the volume and age of water stored in global lakes using a geo-statistical approach. *Nat. Commun.* 7:13603. doi: 10.1038/ncomms13603
- Meyers, P. A., Leenheer, M. J., Eaoie, B. J., and Maule, S. J. (1984). Organic geochemistry of suspended and settling particulate matter in Lake Michigan. *Geochim. Cosmochim. Acta* 48, 443–452. doi: 10.1016/0016-7037(84)90273-4
- Millan, R., Rignot, E., Rivera, A., Martineau, V., Mouginot, J., Zamora, R., et al. (2019). Ice thickness and bed elevation of the Northern and Southern Patagonian Icefields. *Geophys. Res. Lett.* 46, 6626–6635. doi: 10.1029/2019GL082485
- Milner, A. M., Khamis, K., Battin, T. J., Brittain, J. E., Barrand, N. E., Füreder, L., et al. (2017). Glacier shrinkage driving global changes in downstream systems. *Proc. Natl. Acad. Sci. U.S.A.* 114, 9770–9778. doi: 10.1073/pnas.1619807114
- Moffat, C. (2014). Wind-driven modulation of warm water supply to a proglacial fjord, Jorge Montt Glacier, Patagonia. *Geophys. Res. Lett.* 41, 3943–3950. doi: 10.1002/2014GL060071
- Møller, E. F. (2007). Production of dissolved organic carbon by sloppy feeding in the copepods *Acartia tonsa*, *Centropages typicus*, and *Temora longicornis*. *Limnol. Oceanogr.* 52, 79–84. doi: 10.4319/lo.2007.52.1.0079
- Montero, P., Daneri, G., González, H. E., Iriarte, J. L., Tapia, F. J., Lizárraga, L., et al. (2011). Seasonal variability of primary production in a fjord ecosystem of the Chilean Patagonia: implications for the transfer of carbon within pelagic food webs. *Continental Shelf Res.* 31, 202–215. doi: 10.1016/j.csr.2010.09.003
- Montero, P., Pérez-Santos, I., Daneri, G., Gutiérrez, M. H., Igor, G., Seguel, R., et al. (2017). A winter dinoflagellate bloom drives high rates of primary production in a Patagonian fjord ecosystem. *Estuarine Coastal Shelf Sci.* 199, 105–116. doi: 10.1016/j.ecss.2017.09.027
- Mostovaya, A., Hawkes, J. A., Dittmar, T., and Tranvik, L. J. (2017). Molecular determinants of dissolved organic matter reactivity in lake water. *Front. Earth Sci.* 5:106. doi: 10.3389/feart.2017.00106
- Mulholland, M. R., and Lee, C. (2009). Peptide hydrolysis and the uptake of dipeptides by phytoplankton. *Limnol. Oceanogr.* 54, 856–868. doi: 10.4319/lo.2009.54.3.0856
- Murphy, K. R., Stedmon, C. A., Graeber, D., and Bro, R. (2013). Fluorescence spectroscopy and multi-way techniques. PARAFAC. *Anal. Methods* 5:6557. doi: 10.1039/c3ay41160e
- Murphy, K. R., Stedmon, C. A., Waite, T. D., and Ruiz, G. M. (2008). Distinguishing between terrestrial and autochthonous organic matter sources in marine environments using fluorescence spectroscopy. *Mar. Chem.* 108, 40–58.
- Murphy, K. R., Stedmon, C. A., Wenig, P., and Bro, R. (2014). OpenFluor—an online spectral library of auto-fluorescence by organic compounds in the environment. *Anal. Methods* 6, 658–661. doi: 10.1039/C3AY41935E
- Nagata, T., Fukuda, H., Fukuda, R., and Koike, I. (2000). Bacterioplankton distribution and production in deep Pacific waters: large-scale geographic variations and possible coupling with sinking particle fluxes. *Limnol. Oceanogr.* 45, 426–435. doi: 10.4319/lo.2000.45.2.0426
- Ohno, T., He, Z., Sleighter, R. L., Honeycutt, C. W., and Hatcher, P. G. (2010). Ultrahigh resolution mass spectrometry and indicator species analysis to identify marker components of soil- and plant biomass-derived organic matter fractions. *Environ. Sci. Technol.* 44, 8594–8600. doi: 10.1021/es101089t
- Oksanen, J., Blanchet, F. G., Kindt, R., Legendre, P., Minchin, P. R., O'Hara, R. B., et al. (2016). *Vegan: Community Ecology Package. R Package Version 2.2-1*. 2015.
- Osterholz, H., Kirchman, D. L., Niggemann, J., and Dittmar, T. (2016). Environmental drivers of dissolved organic matter molecular composition in the Delaware Estuary. *Front. Earth Sci.* 4:95. doi: 10.3389/feart.2016.00095
- Pace, M. L., Cole, J. J., Carpenter, S. R., Kitchell, J. F., Hodgson, J. R., Van De Bogert, M. C., et al. (2004). Whole-lake carbon-13 additions reveal terrestrial support of aquatic food webs. *Nature* 427, 240–243. doi: 10.1038/nature02227
- Pantoja, S., Luis Iriarte, J., and Daneri, G. (2011). Oceanography of the Chilean Patagonia. *Continental Shelf Res.* 31, 149–153. doi: 10.1016/j.csr.2010.10.013
- Paulsen, M. L., Müller, O., Larsen, A., Møller, E. F., Middelboe, M., Sejr, M. K., et al. (2018). Biological transformation of Arctic dissolved organic matter in a NE Greenland fjord. *Limnol. Oceanogr.* 64, 1014–1033. doi: 10.1002/lno.11091
- Paulsen, M. L., Nielsen, S. E. B., Müller, O., Møller, E. F., Stedmon, C. A., Juul-Pedersen, T., et al. (2017). Carbon bioavailability in a high Arctic fjord influenced by glacial meltwater, NE Greenland. *Front. Mar. Sci.* 4:176. doi: 10.3389/fmars.2017.00176
- Piret, L., Troch, M., Vandekerckhove, E., Harada, N., Moffat, C., Rivera, A., et al. (2019). *Gridded Bathymetry (KMZ format) of the Baker-Martinez fjord complex (Chile, 48°S) v2*. Palisades, NY: Interdisciplinary Earth Data Alliance (IEDA). doi: 10.1594/IEDA/324869
- Poulet, S. A., Williams, R., Conway, D. V. P., and Videau, C. (1991). Co-occurrence of copepods and dissolved free amino acids in shelf sea waters. *Mar. Biol.* 108, 373–385. doi: 10.1007/BF01313646
- Quiroga, E., Ortiz, P., Gerdes, D., Reid, B., Villagran, S., and Quiñones, R. (2012). Organic enrichment and structure of macrobenthic communities in the glacial Baker Fjord, Northern Patagonia, Chile. *J. Mar. Biol. Assoc. U.K.* 92, 73–83. doi: 10.1017/S0025315411000385
- R Core Team (2015). *R: A Language and Environment for Statistical Computing*. Vienna: R Foundation for Statistical Computing.
- Rebolledo, L., Bertrand, S., Lange, C. B., Tapia, F. J., Quiroga, E., Troch, M., et al. (2019). Compositional and biogeochemical variations of sediments across the terrestrial-marine continuum of the Baker-Martinez fjord system (Chile, 48°S). *Prog. Oceanogr.* 174, 89–104. doi: 10.1016/j.poccean.2018.12.004

- RGI Consortium (2017). *Randolph Glacier Inventory – A Dataset of Global Glacier Outlines: Version 6.0. Technical Report, Global Land Ice Measurements from Space*. Denver, CO: Digital Media. doi: 10.7265/N5-RGI-60
- Riedel, T., Zark, M., Vähätalo, A. V., Niggemann, J., Spencer, R. G. M., Hernes, P. J., et al. (2016). Molecular signatures of biogeochemical transformations in dissolved organic matter from ten world rivers. *Front. Earth Sci.* 4:85. doi: 10.3389/feart.2016.00085
- Rivera, A., Corripio, J., Bravo, C., and Cisternas, S. (2012). Glacier Jorge Montt (Chilean Patagonia) dynamics derived from photos obtained by fixed cameras and satellite image feature tracking. *Ann. Glaciol.* 53, 147–155. doi: 10.3189/2012AoG60A152
- Romera-Castillo, C., Sarmiento, H., Álvarez-Salgado, X. A., Gasol, J. M., and Marrasé, C. (2010). Production of chromophoric dissolved organic matter by marine phytoplankton. *Limnol. Oceanogr.* 55, 446–454. doi: 10.4319/lo.2010.55.1.0446
- Romera-Castillo, C., Sarmiento, H., Alvarez-Salgado, X. A. Á, Gasol, J. M., and Marrasé, C. (2011). Net production and consumption of fluorescent colored dissolved organic matter by natural bacterial assemblages growing on marine phytoplankton exudates. *Appl. Environ. Microbiol.* 77, 7490–7498. doi: 10.1128/AEM.00200-11
- Ross, L., Pérez-Santos, I., Valle-Levinson, A., and Schneider, W. (2014). Semidiurnal internal tides in a Patagonian fjord. *Prog. Oceanogr.* 129, 19–34. doi: 10.1016/j.pocean.2014.03.006
- Saldias, G. S., Sobarzo, M., and Quiñones, R. (2019). Freshwater structure and its seasonal variability off western Patagonia. *Prog. Oceanogr.* 174, 143–153. doi: 10.1016/j.pocean.2018.10.014
- Seidel, M., Manecki, M., Herlemann, D. P. R., Deutsch, B., Schulz-Bull, D., Jürgens, K., et al. (2017). Composition and transformation of dissolved organic matter in the Baltic Sea. *Front. Earth Sci.* 5:31. doi: 10.3389/feart.2017.00031
- Shimotori, K., Omori, Y., and Hama, T. (2010). Bacterial production of marine humic-like fluorescent dissolved organic matter and its biogeochemical importance. *Aquatic Microb. Ecol.* 58, 55–66. doi: 10.3354/ame01350
- Sholkovitz, E. R. (1976). Flocculation of dissolved organic and inorganic matter during the mixing of river water and seawater. *Geochim. Cosmochim. Acta* 40, 831–845. doi: 10.1016/0016-7037(76)90035-1
- Singer, G. A., Fasching, C., Wilhelm, L., Niggemann, J., Steier, P., Dittmar, T., et al. (2012). Biogeochemically diverse organic matter in Alpine glaciers and its downstream fate. *Nat. Geosci.* 5, 710–714. doi: 10.1038/ngeo1581
- Sleighter, R. L., and Hatcher, P. G. (2008). Molecular characterization of dissolved organic matter (DOM) along a river to ocean transect of the lower Chesapeake Bay by ultrahigh resolution electrospray ionization Fourier transform ion cyclotron resonance mass spectrometry. *Mar. Chem.* 110, 140–152. doi: 10.1016/j.marchem.2008.04.008
- Smith, D. F., Podgorski, D. C., Rodgers, R. P., Blakney, G. T., and Hendrickson, C. L. (2018). 21 tesla FT-ICR mass spectrometer for ultrahigh-resolution analysis of complex organic mixtures. *Anal. Chem.* 90, 2041–2047. doi: 10.1021/acs.analchem.7b04159
- Smith, R. W., Bianchi, T. S., Allison, M., Savage, C., and Galy, V. (2015). High rates of organic carbon burial in fjord sediments globally. *Nat. Geosci.* 8, 450–453. doi: 10.1038/ngeo2421
- Spencer, R. G. M., Stubbins, A., Hernes, P. J., Baker, A., Mopper, K., Aufdenkampe, A. K., et al. (2009). Photochemical degradation of dissolved organic matter and dissolved lignin phenols from the Congo River. *J. Geophys. Res. Biogeosci.* 114:G03010. doi: 10.1029/2009JG000968
- Spencer, R. G. M. M., Guo, W., Raymond, P. A., Dittmar, T., Hood, E., Fellman, J., et al. (2014). Source and biolability of ancient dissolved organic matter in glacier and lake ecosystems on the tibetan plateau. *Geochim. Cosmochim. Acta* 142, 64–74. doi: 10.1016/j.gca.2014.08.006
- Stubbins, A., Spencer, R. G. M., Chen, H., Hatcher, P. G., Mopper, K., Hernes, P. J., et al. (2010). Illuminated darkness: molecular signatures of Congo River dissolved organic matter and its photochemical alteration as revealed by ultrahigh precision mass spectrometry. *Limnol. Oceanogr.* 55, 1467–1477. doi: 10.4319/lo.2010.55.4.1467
- Sun, L., Perdue, E. M., Meyer, J. L., and Weis, J. (1997). Use of elemental composition to predict bioavailability of dissolved organic matter in a Georgia river. *Limnol. Oceanogr.* 42, 714–721. doi: 10.4319/lo.1997.42.4.0714
- Tateishi, R., Hoan, N. T., Kobayashi, T., Alsaadeh, B., Tana, G., and Phong, D. X. (2014). Production of Global Land Cover Data – GLCNMO2008. *J. Geogr. Geol.* 6, 99–122. doi: 10.5539/jgg.v6n3p99
- Urban-Rich, J., McCarty, J. T., and Shailer, M. (2004). Effects of food concentration and diet on chromophoric dissolved organic matter accumulation and fluorescent composition during grazing experiments with the copepod *Calanus finmarchicus*. *ICES J. Mar. Sci.* 61, 542–551. doi: 10.1016/j.icesjms.2004.03.024
- Vargas, C. A., Martinez, R. A., San Martin, V., Aguayo, M., Silva, N., and Torres, R. (2011). Allochthonous subsidies of organic matter across a lake–river–fjord landscape in the Chilean Patagonia: implications for marine zooplankton in inner fjord areas. *Continental Shelf Res.* 31, 187–201. doi: 10.1016/j.csr.2010.06.016
- Ward, N. D., Bianchi, T. S., Medeiros, P. M., Seidel, M., Richey, J. E., Keil, R. G., et al. (2017). Where carbon goes when water flows: carbon cycling across the aquatic continuum. *Front. Mar. Sci.* 4:7. doi: 10.3389/fmars.2017.00007
- Welti, N., Striebel, M., Ulseth, A. J., Cross, W. F., DeVilbiss, S., Glibert, P. M., et al. (2017). Bridging food webs, ecosystem metabolism, and biogeochemistry using ecological stoichiometry theory. *Front. Microbiol.* 8:1298. doi: 10.3389/fmicb.2017.01298
- Włodarska-Kowalczyk, M., Mazurkiewicz, M., Górska, B., Michel, L. N., Jankowska, E., and Zaborska, A. (2019). Organic carbon origin, benthic faunal consumption, and burial in sediments of Northern Atlantic and Arctic Fjords (60–81°N). *J. Geophys. Res. Biogeosci.* 124, 3737–3751. doi: 10.1029/2019JG005140
- Yamashita, Y., Fichot, C. G., Shen, Y., Jaffé, R., and Benner, R. (2015). Linkages among fluorescent dissolved organic matter, dissolved amino acids and lignin-derived phenols in a river-influenced ocean margin. *Front. Mar. Sci.* 2:92. doi: 10.3389/fmars.2015.00092
- Yamashita, Y., Jaffé, R., Maie, N., and Tanoue, E. (2008). Assessing the dynamics of dissolved organic matter (DOM) in coastal environments by excitation emission matrix fluorescence and parallel factor analysis (EEM-PARAFAC). *Limnol. Oceanogr.* 53, 1900–1908. doi: 10.4319/lo.2008.53.5.1900
- Zemp, M., Frey, H., Gärtner-Roer, I., Nussbaumer, S. U., Hoelzle, M., Paul, F., et al. (2015). Historically unprecedented global glacier decline in the early 21st century. *J. Glaciol.* 61, 745–762. doi: 10.3189/2015JoG15J017
- Zhu, Z. Y., Wu, Y., Liu, S. M., Wenger, F., Hu, J., Zhang, J., et al. (2016). Organic carbon flux and particulate organic matter composition in Arctic valley glaciers: examples from the Bayelva River and adjacent Kongsfjorden. *Biogeosciences* 13, 975–987. doi: 10.5194/bg-13-975-2016

**Conflict of Interest:** The authors declare that the research was conducted in the absence of any commercial or financial relationships that could be construed as a potential conflict of interest.

Copyright © 2021 Marshall, Kellerman, Wadham, Hawkings, Daneri, Torres, Pryer, Beaton, Ng, Urra, Robinson and Spencer. This is an open-access article distributed under the terms of the Creative Commons Attribution License (CC BY). The use, distribution or reproduction in other forums is permitted, provided the original author(s) and the copyright owner(s) are credited and that the original publication in this journal is cited, in accordance with accepted academic practice. No use, distribution or reproduction is permitted which does not comply with these terms.